Published in final edited form as:

*Nature*. 2016 June 30; 534(7609): 700–704. doi:10.1038/nature18310.

# Coordinating cardiomyocyte interactions to direct ventricular chamber morphogenesis

**Peidong Han**[1], **Joshua Bloomekatz**[1], **Jie Ren**[1], **Ruilin Zhang**[1], **Jonathan D. Grinstein**[1], **Long Zhao**[2], **C. Geoffrey Burns**[2], **Caroline E. Burns**[2], **Ryan M. Anderson**[3], and **Neil C. Chi**[1,4,*]

[1]Department of Medicine, Division of Cardiology, University of California, San Diego, La Jolla, CA 92093, USA

[2]Cardiovascular Research Center, Division of Cardiology, Department of Medicine, Massachusetts General Hospital and Harvard Medical School, Charlestown, MA 02129

[3]Center for Diabetes and Metabolic Diseases, Department of Pediatrics and Department of Cellular and Integrative Physiology, Indiana University School of Medicine, Indianapolis, IN, 46202.

[4]Institute of Genomic Medicine, University of California, San Diego, La Jolla, CA 92093, USA

## Abstract

Many organs are composed of complex tissue walls that are structurally organized to optimize organ function. In particular, the ventricular myocardial wall of the heart is comprised of an outer compact layer that concentrically encircles the ridge-like inner trabecular layer. Although disruption in the morphogenesis of this myocardial wall can lead to various forms of congenital heart disease (CHD)[1] and non-compaction cardiomyopathies[2], it remains unclear how embryonic cardiomyocytes assemble to form ventricular wall layers of appropriate spatial dimensions and myocardial mass. Here, we utilize advanced genetic and imaging tools in zebrafish to reveal an interplay between myocardial Notch and Erbb2 signaling that directs the spatial allocation of myocardial cells to their proper morphologic positions in the ventricular wall. Although previous studies have shown that endocardial Notch signaling non-cell-autonomously promotes myocardial trabeculation through Erbb2 and BMP signaling[3], we discover that distinct ventricular cardiomyocyte clusters exhibit myocardial Notch activity that cell-autonomously inhibits Erbb2 signaling and prevents cardiomyocyte sprouting and trabeculation. Myocardial-specific Notch inactivation leads to ventricles of reduced size and increased wall thickness due to excessive trabeculae, whereas widespread myocardial Notch activity results in ventricles of increased size with a single-cell thick wall but no trabeculae. Notably, this myocardial Notch signaling is activated non-cell-autonomously by neighboring Erbb2-activated cardiomyocytes that sprout and



*To whom correspondence should be addressed. nchi@ucsd.edu, 858-822-1842.

**Author Contributions:** P.H. and N.C.C. conceived the project and the design of the experimental strategy. P.H., J.R., J.B., R.Z., and J.D.G. conducted experiments. L.Z. generated the *ubi:*RSdnM transgenic line. P.H. and N.C.C. generated and characterized *myl7:*Cre transgenic line. C.E.B, C.G.B, and R.A.M. provided key reagents. P.H., J.B. and N.C.C. prepared the manuscript.

The authors declare no competing financial interests.

form nascent trabeculae. Thus, these findings support an interactive cellular feedback process that guides the assembly of cardiomyocytes to morphologically create the ventricular myocardial wall and more broadly provides insight into the cellular dynamics of how diverse cell lineages organize to create form.

---

The embryonic zebrafish heart is comprised of 200-300 cardiomyocytes when cardiac chambers form[4], and thus provides an opportunity to interrogate in detail how individual cardiomyocytes organize to create the nascent structures of the vertebrate embryonic ventricular wall. As a result, previous zebrafish studies have shown that distinct cardiomyocytes extend from the embryonic ventricular wall into the lumen to develop cardiac trabeculae[5], whereas others remain within this outer wall to create the primordial layer[4]. Yet, how these cardiomyocytes are selected to form the distinct myocardial layers of the ventricular wall remains to be fully elucidated.

Because of the role of Notch signaling in regulating cell-cell interactions[6,7], we examined its dynamic activation during zebrafish embryonic ventricular morphogenesis utilizing the *Tg(Tp1:d2GFP)* Notch reporter line, which expresses a destabilized fluorescent protein upon Notch activation[8] (Fig. 1, Extended Data Fig. 1). As previously reported[9], we observed Notch signaling first in the ventricular endocardium at 24 hpf (hours post-fertilization), which then becomes restricted to the atrioventricular (AV) and outflow tract (OFT) endocardium at 48 hpf (Extended Data Fig. 1a-l). From 72-96 hpf when cardiac trabeculation initiates[5,10,11], a subset of ventricular cardiomyocytes begins to express Notch-activated *Tp1:*d2GFP and remains in the ventricular outer wall (Fig. 1a-h, arrows, Extended Data Fig. 1m-o, arrows), whereas ventricular cardiomyocytes extending to form cardiac trabeculae fail to express *Tp1:*d2GFP (Fig. 1a-h arrowheads). These *Tp1:*d2GFP$^{+}$ cardiomyocytes are frequently adjacent to sprouting *Tp1:*d2GFP$^{-}$ cardiomyocytes (Fig. 1a-h) and form clusters of 2-3 cardiomyocytes across the surface of the ventricular myocardial wall (Fig. 1m-t), which quantitatively correlate with the number of emerging cardiac trabeculae (Extended Data Fig. 1p-r). However, after the heart has established cardiac trabeculae, these *Tp1:*d2GFP$^{+}$ myocardial clusters progressively decrease and are no longer observed by 14 dpf (days post-fertilization), despite the presence of *Tp1:*d2GFP$^{+}$ AV and OFT endocardial cells (Fig. 1i-l, o, p, s, t, Extended Data Fig. 1s, t).

Using the *Tg(Tp1:eGFP)* Notch reporter line[12], which expresses a more stable fluorescent protein compared to *Tg(Tp1:d2GFP)* (Extended Data Fig. 2a-h), we observed that *Tp1:*eGFP$^{+}$ cardiomyocytes remain present in the ventricular outer wall until 30-45 dpf due to the eGFP perdurance, and then become the ventricular primordial layer by 60-90 dpf when the ventricular cortical layer of the adult zebrafish heart forms[4] (Extended Data Fig. 3a-n). Unlike ventricular trabecular and cortical cardiomyocytes, these *Tp1:*eGFP$^{+}$ ventricular primordial cardiomyocytes fail to display organized sarcomeres by α-actinin immunostaining, are surrounded by extensive wheat germ agglutinin (WGA) stained extracellular matrix and exhibit a thin cellular morphology as previously reported[4] (Extended Data Fig. 3o-t). Overall, these data suggest that early myocardial Notch signaling may determine which ventricular cardiomyocytes remain in the embryonic ventricular outer

wall to subsequently become the distinctive ventricular primordial layer of the adult zebrafish heart.

We next investigated the role of Notch signaling in the endocardium and myocardium during ventricular morphogenesis through selectively perturbing Notch signaling at specific cardiac developmental stages. Treating zebrafish embryos with DAPT, which effectively decreases *Tp1:*d2GFP Notch reporter expression and inhibits Notch signaling (Extended Data Fig. 2), from 20-48 hpf when Notch signaling is activated in the endocardium, reduces cardiac trabeculation (Extended Data Fig. 2q-s) as previously described[3]; however, treating from 60-72 hpf when Notch signaling is present in the ventricular myocardium, results in increased trabeculae formation (Fig. 2a, b, i, j). Consistent with these results, BMP signaling, which is activated in ventricular trabeculae[3], is also increased in similarly DAPT-treated zebrafish embyros from 60-72 hpf (Extended Data Fig. 4a-f). Furthermore, heat-shocking *Tg(hsp70l:dnMAML-GFP)*[13] - *hsp70l:dnM* embryos from 60-72 hpf, which induces dominant negative Mastermind-like (dnMAML) expression to block downstream Notch signaling, results in similar excessive trabeculation (Fig. 2c, d, k, l).

To explore whether Notch signaling functions in a cardiomyocyte-specific manner to directly guide myocardial cell fate position within the ventricle, we employed a myocardial-specific Cre (Extended Data Fig. 5a-d) strategy in combination with *Tg(ubi:loxp-mKate2-STOP-loxp-dnMAML-GFP)* or *Tg(hsp70l:loxp-mCherry-STOP-loxp-NICD-P2A-emerald)*[14] "switch lines" (abbreviated as *ubi:RSdnM* and *hsp70l:RSN*) to inhibit or activate Notch signaling in cardiomyocytes, respectively. As observed in DAPT-treated and heat-shocked *Tg(hsp70l:dnM)* zebrafish from 60-72 hpf, *Tg(myl7:Cre; ubi:RSdnM)* zebrafish display excessive cardiac trabeculation due to inhibition of myocardial Notch signaling (Fig. 2e, f, m, n). Conversely, heat-shocking *Tg(myl7:Cre; hsp70l:RSN)* zebrafish, which induces myocardial Notch-intracellular domain (NICD) expression, between 60-120 hpf leads to cardiac ventricles without significant trabeculae because of constitutively-activated Notch signaling throughout the myocardium (Fig. 2g, h, o, p). Moreover, constitutive myocardial Notch activation at later time points (80-, 96-, and 120- hpf to 7 dpf) prevents trabeculae from further sprouting and/or extending (Extended Data Fig. 6a-g); however, trabeculae continue to develop after the cessation of this myocardial Notch activity, but fail to recover to wild-type levels (Extended Data Fig. 6h, i).

In line with these findings, we discovered that Notch inhibition results in smaller ventricular areas (Fig. 2a-f, Extended Data Fig. 5e) and thicker ventricular myocardial walls (Fig. 2a-f, Extended Data Fig. 5f) due to increased cardiomyocytes within the trabecular layer (~2-3 cells thick) (Fig. 2i-n, Extended Data Fig. 5g), whereas Notch activation gives rise to larger ventricular areas (Fig. 2g, h, Extended Data Fig. 5e) and thinner ventricular myocardial walls (Fig. 2g, h, Extended Data Fig. 5f) that are ~one cell thick with no apparent trabecular cardiomyocytes (Fig. 2o, p, Extended Data Fig. 5g). Although these hearts do not exhibit a significant difference in overall cardiomyocyte numbers compared to control hearts (Extended Data Fig. 5h-p), we did discover that Notch inhibition promotes the redistribution of N-cadherin away from intercellular contacts while Notch activation prevents this reorganization (Extended Data Fig. 7), suggesting that myocardial Notch signaling may control ventricular size and wall thickness through regulating the allocation of

cardiomyocytes between the ventricular wall layers via cell-cell contacts. To further investigate this possibility, we monitored the fate of individual genetically labeled cardiomyocytes using a myocardial specific Brainbow system *Tg(myl7:CreER; priZm)*[4] (Fig. 2q-t). After confirming that adjacent cardiomyocytes were consistently labeled with different colors at 60 hpf prior to trabeculation (Extended Data Fig. 8), we treated zebrafish embryos with DAPT or DMSO from 60-72 hpf. DAPT treatment leads to increased numbers of trabeculating clones and conversely decreased numbers of non-trabeculating clones when compared to DMSO-treated hearts; however, the total number of ventricular cardiomyocyte clones is not significantly different (Fig. 2r-t), further supporting that Notch signaling segregates individual cardiomyocyte clones between the ventricular outer wall and inner trabecular layers.

To examine whether Notch signaling acts cell-autonomously to control cardiomyocyte sprouting, we perturbed Notch signaling in individual cardiomyocytes during trabeculation by injecting *hsp70l:loxp-mCherry-STOP-loxp-NICD-P2A-emerald* (*hsp70l:RSN* - Notch activating) or *hsp70l:loxp-mCherry-STOP-loxp-dnSuH-P2A-emerald*[15] (*hsp70l:RSdnS* - dominant negative Suppressor of Hairless/Notch repressing) switch plasmids into *Tg(myl7:Cerulean)*[16]*; Tg(myl7:Cre)* zebrafish embryos (Fig. 2u). Heat-shocking these injected fish from 60-72 hpf resulted in the majority of Notch-activated NICD-P2A-Emerald$^+$ cardiomyocytes remaining in the ventricular outer myocardial wall (Fig. 2w, z), whereas Notch-inhibited dnSuH-P2A-Emerald$^+$ cardiomyocytes reside primarily in trabeculae (Fig. 2y, z). Heat-shocking injected control fish lacking *Tg(myl7:Cre)* generated mCherry$^+$ cardiomyocytes that are distributed equally between both myocardial layers (Fig. 2v, x, z), altogether revealing a myocardial cell-autonomous role for Notch signaling.

Because Neuregulin/Erbb2 and BMP10 signaling can promote cardiac trabeculation[3,10,17], we investigated whether myocardial Notch may cross-talk with these signaling pathways to regulate cardiomyocyte selection between the ventricular wall layers. Inhibiting Erbb2 signaling with AG1478 treatment[10] from 60-72 hpf prevents cardiac trabeculation and expression of *Tp1:*d2GFP in cardiomyocytes although *Tp1:*d2GFP remains expressed in AV and OFT endocardial cells (Extended Data Fig. 9a, b). Consistent with these findings, both *erbb2* morpholino (MO) knockdown and *erbb2* −/− mutant (*erbb2*$^{st50}$) *Tg(Tp1:d2GFP)* embryos, which exhibit similar trabecular defects[10,18], also fail to display Notch reporter expression in the myocardium (Fig. 3a, b, d), supporting a requirement for Erbb2 signaling in the initiation of trabeculation and the activation of myocardial Notch signaling. Notably, neither DAPT treatment nor heat-shock induction of dnMAML between 60-72 hpf, which alone increases trabeculation (Fig. 2), could rescue the relative lack of cardiac trabeculae in loss of Erbb2 function zebrafish (Fig. 3c, e, Extended Data Fig. 9b-e). In contrast to the Erbb2 loss of function findings, BMP inhibited embryos using Dorsomorphin[19] from 60-72 hpf form cardiac trabeculae and express myocardial *Tp1:*d2GFP (Extended Data Fig. 4m-p) despite the abrogation of the BMP-reporter, *BRE:*d2GFP in the trabecular layer (Extended Data Fig. 4j-l). However, by 7 dpf, these hearts display aberrant and stunted cardiac trabeculae compared to DMSO-treated fish (Extended Data Fig. 4q-s), corroborating a requirement for BMP signaling in the maintenance but not the initiation of cardiac trabeculation[20].

To explore whether Notch activation negatively regulates Erbb2 signaling to prevent trabeculae formation, we examined *erbb2* expression in 72 hpf *Tp1*:d2GFP hearts and discovered that *erbb2* is expressed in many ventricular cardiomyocytes but diminished in *Tp1*:d2GFP$^{+}$ cardiomyocytes (Extended Data Fig. 9f-j). In support of these findings, constitutive myocardial Notch activation by heat-shocking *Tg(myl7:Cre; hsp70l:RSN)* fish between 60-120 hpf results in the dramatic reduction of *erbb2* myocardial expression (Extended Data Fig. 9k, l, o, p). In contrast, Notch-inhibited hearts treated with DAPT from 60-72 hpf exhibit increased *erbb2* myocardial expression (Extended Data Fig. 9m, n, q, r). Thus, myocardial Notch signaling may block Neuregulin/Erbb2 signaling by down-regulating *erbb2* expression to inhibit cardiomyocyte sprouting.

Since Notch signaling has been shown to mediate cell fate position through lateral inhibition mechanisms[6,7,21,22], we investigated whether Erbb2 signaling non-cell-autonomously activates myocardial Notch signaling in neighboring cardiomyocytes. Thus, we created mosaic embryos by transplanting *Tg(myl7:Cerulean)* wild-type donor blastomeres into *erbb2* or control MO injected *Tg(Tp1:d2GFP); Tg(myl7:H2A-mCherry)*[23] host embryos and assessed the ability of wild-type donor cells to contribute to the ventricular wall layers and activate myocardial Notch signaling. As previously reported[10], a greater percentage of donor-derived wild-type cardiomyocytes is present in the trabeculae of *erbb2* knockdown embryos compared to control embryos (compare Fig. 3i to 3g, Extended Data Fig. 10a). Although non-transplanted *erbb2* knockdown hearts fail to exhibit myocardial Notch activity (Fig. 3f, h), transplanted *erbb2* knockdown host hearts containing wild-type donor myocardial cells (*myl7*:Cerulean$^{+}$) can activate myocardial *Tp1*:d2GFP expression (Fig. 3i, Extended Data Fig. 10b). Upon closer inspection, these host *erbb2* knockdown *Tp1*:d2GFP$^{+}$ cardiomyocytes (Fig. 3i arrows) appear adjacent to donor wild-type *myl7*:Cerulean$^{+}$ cardiomyocytes (Fig. 3i arrowheads, Extended Data Fig. 10c), supporting a role for Erbb2 responsive cardiomyocytes in activating Notch signaling in neighboring cardiomyocytes.

Based on these results, we searched for potential Notch ligands mediating the activation of Notch signaling in neighboring cardiomyocytes and discovered that *jag2b* is expressed in select ventricular cardiomyocytes at 72 hpf when myocardial Notch signaling is activated (Fig. 4a, b). This ventricular myocardial *jag2b* expression is reduced in *erbb2* −/− mutant hearts (Fig. 4c, d), suggesting that Erbb2 signaling may activate Notch signaling in neighboring cardiomyocytes through *jag2b*. In support of this possibility, we discovered that *jag2b* −/− mutant hearts exhibit not only increased trabeculation as observed in Notch-inhibited hearts but also reduced *Tp1*:d2GFP Notch reporter activity in the ventricular myocardium but not in the AV or OFT endocardium (Fig. 4e-h). Together these data support a model in which myocardial Erbb2 signaling non-cell-autonomously activates Notch signaling in neighboring ventricular outer wall cardiomyocytes through Jag2b, which in turn leads to the reduction of *erbb2* expression, subsequent inhibition of Erbb2 signaling, and suppression of cardiomyocyte sprouting (Fig. 4i-k).

Overall, these findings reveal a molecular mechanism whereby Notch and Erbb2 signaling coordinates social cellular interactions between cardiomyocytes that determine their morphologic fate within the ventricular wall. Although previous studies have suggested that Notch signaling may be activated in the myocardium[24-27], our zebrafish studies illuminate

the precise role of myocardial Notch activity in forming the ventricular wall. Similar to the receptor tyrosine kinase (RTK)-Notch lateral inhibition signaling mechanisms that regulate epithelial tip and stalk cell formation during branching morphogenesis[6,7], myocardial Notch acts in concert with the RTK, Erbb2, to segregate embryonic cardiomyocytes into two functionally distinct classes of cells: 1) sprouting cardiomyocytes which respond to Neuregulin via Erbb2 and 2) non-sprouting Notch-activated cardiomyocytes, in which Notch signaling inhibits *erbb2* expression. These roles appear to not be pre-specified, but rather are determined by social interactions between cardiomyocytes. Furthermore, recent studies have reported human Notch genetic variants linked to a wide spectrum of CHDs including non-compaction cardiomyopathies[28,29], which exhibit similar severe ventricular wall defects to those observed in our Notch studies. More broadly, our studies support a conserved role for intercellular cross-talk between RTKs and Notch signaling for allocating cells within organ substructures and may be particularly relevant in developing strategies for human pluripotent stem cell tissue-specific developmental and disease modeling or regenerative therapies.

## Methods

### Zebrafish husbandry and strains

Zebrafish (*Danio rerio*) were raised under standard laboratory conditions at 28°C. All animal work was approved by the University of California at San Diego Institutional Animal Care and Use Committee (IACUC). The following established transgenic and mutant lines were used: *Tg(EPV.Tp1-Mmu.Hbb:d2GFP)*$^{mw43}$([8]) abbreviated as *Tg(Tp1:d2GFP)*; *Tg(EPV.Tp1-Mmu.Hbb:eGFP)*$^{um14}$([12]) abbreviated as *Tg(Tp1:eGFP)*; *Tg(BRE-AAVmlp:d2GFP)*$^{mw30}$([19]) abbreviated as *Tg(BRE:d2GFP)*; *Tg(hsp70l:dnMAML-GFP)*$^{fb10}$([13]) abbreviated as *Tg(hsp70l:dnM)*; *Tg(kdrl:ras-mCherry)*$^{S896}$([30]); *Tg(myl7:H2A-mCherry)*$^{sd12}$([23]); *Tg(myl7:mCherry)*$^{sd7}$([31]); *Tg(myl7:Cerulean)*$^{co19}$([16]); *Tg(myl7:eGFP-HRAS)*$^{s883}$([32]) abbreviated as *Tg(myl7:ras-eGFP)*; *Tg(myl7:CreER)*$^{pd10}$([33]); *Tg(β-act2:Brainbow1.0L)*$^{pd49}$([4]) abbreviated as *Tg(priZm)*; Tg(hsp70l:loxp-mCherry-STOP-loxp-NICD-P2A-emerald)$^{S961}$ ([14]) abbreviated as *Tg(hsp70l:RSN)*; *Tg(β-act2:loxP-DsRed-STOP-loxP-eGFP)*$^{s928}$([33]) abbreviated as *Tg(β-act2:RSG)*; *erbb2*$^{st50}$([18]) and *jag2b*$^{hu3425}$ ([34]).

To generate the *Tg(myl7:Cre)*$^{sd38}$ transgenic line, a 900 bp fragment of the *myl7* promoter[35] was cloned upstream of the *Cre* recombinase gene into a multi-cloning site flanked by I-SceI sites in the pBluescript-SK vector. Standard I-SceI meganuclease transgenesis[36] was used to create transgenic founders which were screened for myocardial Cre recombinase activity by crossing to the *Tg(β-act2:RSG)*$^{s928}$ line. Three independent founders were identified, all with similar levels of Cre recombinase activity and matching the expression of *Tg(myl7:Cerulean)*$^{co19}$ (Extended Data Fig. 5a-d). A single representative founder was propagated further.

To generate the *Tg(ubi:loxp-mKate2-STOP-loxp-dnMAML-GFP)*$^{fb16}$ strain, abbreviated as *Tg(ubi:RSdnM),* gateway cloning technology (Life Technologies) was used to conduct an LR recombination reaction with the *pENTR5'_ubi*[37], *pME-loxp-mKate2-STOP-loxp*, *p3E-dnMAML-GFP* entry vectors and the *pDESTol2pA2* destination vector[38]. The *pME-loxp-mKate2-STOP-loxp* entry vector was created by replacing the *AmCyan* cDNA in the *pME-*

*loxp-AmCyan-STOP-loxp*[39] vector with a cDNA encoding mKate2 (Evrogen) using In-Fusion HD cloning (Clontech Laboratories Inc.). The *p3E-dnMAML-GFP* entry vector was generated by conducting a BP recombination reaction between a PCR product encoding a fusion protein between dnMAML and GFP amplified from *pME-dnMAML-GFP*[13] and the Gateway Donor Vector *pDONRP2R-P3*. Altogether the *ubi:loxp-mKate2-STOP-loxp-dnMAML-GFP* construct was co-injected with Tol2 transposase mRNA[38] into 1-cell stage embryos to generate independent founders which were screened for mKate2 and then GFP upon Cre-mediated recombination. Founders with both mKate2 and GFP were propagated further.

## Embryonic immunofluorescence and live imaging studies

Whole mount immunofluorescence studies were performed as previously described[40], with the following modifications. After initial fixation, any pre-existing fluorescence was quenched by incubating embryos in 2M HCl at 37°C for 30 min and washing with $ddH_2O$ and phosphate buffer saline with 0.1% Tween-20 (PBST). The antibodies used were anti-Mef2/C-21 (rabbit, Santa Cruz Biotechnology, 1:100), anti-MHC/MF20 (mouse, Developmental Studies Hybridoma Bank, 1:100) or anti-N-cadherin (rabbit, GeneTex, 1:100) followed by anti-rabbit IgG-Alexa 488 (goat, Life Technologies 1:200).

For embryonic studies of Notch activity, embryos containing the Notch reporters *Tg(Tp1:d2GFP)*$^{mw43}$ or *Tg(Tp1:eGFP)*$^{um14}$ in combination with myocardial-expressed transgenes such as *Tg(myl7:mCherry)*$^{sd7}$ or endothelial expressed transgenes such as *Tg(kdrl:ras-mCherry)*$^{S896}$ were imaged live[40]. The *Tp1* promoter used in these Notch reporter transgenics consists of 12 RPBJ-binding sites and reports Notch activity throughout the embryo as previously published[8,12]. These embryos were embedded in 1% low melting agarose (Lonza) in a coverslip bottom culture dish (MatTek) and cardiac contraction was arrested using Tricaine-S (Sigma MS-222) just prior to imaging.

To count the number of *Tp1:*d2GFP$^+$ clusters in each heart, we used 3D reconstructions (Nikon NIS Elements software) from confocal stacks of *Tg(Tp1:d2GFP; myl7:mCherry)* embryos (5-16 hearts per stage). To count the number of cardiomyocytes per *Tp1:*d2GFP$^+$ cluster, *Tg(Tp1:d2GFP; myl7:H2A-mCherry)* embryos were used. Only cells expressing both H2A-mCherry and d2GFP were counted. We analyzed 5-10 hearts per stage to obtain the average number of cardiomyocytes in each *Tp1:*d2GFP cluster at each specified stage. Statistical analysis is described in the Image processing and Statistical analysis section below.

To assess the correlation between nascent trabeculae and *Tp1:*d2GFP$^+$ clusters at 72 hpf, trabeculae were identified in consecutive slices from a Z-stack and pseudo-colored with magenta. A 3D reconstruction was then used to generate the full view of the ventricle, where the number of nascent trabeculae and *Tp1:*d2GFP$^+$ clusters could be counted in each heart. This data is represented in a scatter plot (Extended Data Fig. 1r) and used to overlay a linear regression line.

### Adult immunofluorescence and imaging studies

Immunofluorescence studies were conducted on cryosections of adult zebrafish hearts. These hearts were cryoprotected, mounted, sectioned and stained as performed previously[40]. The following primary antibodies were used: anti-MHC/MF20 (mouse, Developmental Studies Hybridoma Bank, 1:100); anti-α–actinin (mouse, Diagnostic BioSystems, 1:100); anti-Raldh2 (rabbit, Abmart, 1:100); and anti-GFP (chicken, Aves Labs, 1:200). The following secondary antibodies were used: anti-mouse IgG-Alexa 405 (goat, Life technologies, 1:200), anti-mouse IgG-Alexa 594 (goat, Life Technologies, 1:200), anti-rabbit IgGAlexa 568 (goat, Life Technologies, 1:200) and anti-chicken IgG-Alexa 488 (goat, Life Technologies, 1:200). Alexa Fluor 594 conjugated wheat germ agglutinin (WGA) (Life Technologies, 50μg/ml) was used to stain the extracellular matrix. DAPI (1 μg/ml) staining was used to identify nuclei. Notably, we discovered that eGFP from the *Tg(Tp1:eGFP)*$^{um14}$ transgene perdured for a longer period in the ventricular outer myocardial wall (Extended Data Fig. 3) compared to d2GFP from the *Tg(Tp1:d2GFP)*$^{mw43}$ transgene (Extended Data Fig. 1).

### Notch signaling studies

Notch inhibition studies were carried out using: DAPT (a chemical inhibitor of γ-secretase) or dnMAML mis-expression (dominant negative mastermind-like 1). DAPT: Zebrafish embryos were incubated in 100 μM DAPT (Sigma) or 0.1% Dimethyl sulfoxide (DMSO) alone (control) at specified developmental stages and time intervals and then quickly washed (2-3x) with egg water (60 μg/ml Instant Ocean sea salts) for further analysis. The ability of 100 μM DAPT treatment to inhibit Notch signaling was validated by examining *Tp1:*d2GFP expression after DAPT treatment (Extended Data Fig. 2i-p). dnMAML: The *Tg(hsp70l:dnMAML-GFP)* was used to globally express dnMAML at specified time points. Heat-shock induction was conducted by placing *Tg(hsp70l:dnMAML-GFP)* or wild type siblings into a 37°C incubator for 30 min, followed by 3 min in a 42°C water bath. Embryos were heat-shocked twice every 24 hrs to maintain the induction of dnMAML-GFP throughout the embryo. This protocol was highly efficient at inducing dnMAML-GFP expression and produced minimal lethality. To inhibit Notch signaling in cardiomyocytes only, the *Tg(ubi:loxp-mKate2-STOP-loxp-dnMAML-GFP)* line was crossed with the *Tg(myl7:Cre)* line to produce embryos which express dnMAML-GFP only in the myocardium. Induction of dnMAML-GFP was verified by examining GFP fluorescence 5-6 hrs after heat shock or Cre-mediated recombination[13].

Notch activation was carried out by expressing the intracellular domain of Notch1 (NICD). Heat shocking embryos containing both *Tg(hsp70l:loxp-mCherry-STOP-loxp-NICD-P2A-emerald)* ([14]) and *Tg(myl7:Cre)* transgenes produced NICD-P2A-emerald only in the myocardium. Heat shock was carried out as described above.

Ventricular wall thickness was measured to quantify the effect of perturbing Notch signaling and was determined by drawing five representative lines perpendicular to the ventricular wall in a representative confocal slice. Thickness was measured as the distance along the line between the lateral and medial edge of the myocardial wall. All hearts were imaged in

the same orientation and comparable confocal slices were chosen for analysis. Six hearts were measured for each condition.

To determine the effect of altering Notch signaling on cardiomyocyte cell numbers within the ventricular outer wall and trabecular layers, ventricular cardiomyocyte nuclei were counted from hearts exposed to specified experimental conditions using 3D reconstructions of confocal slices from embryos with *myl7:*H2A-mCherry or from embryos stained with the Mef2 antibody. Mef2 immunostaining was used in embryos containing transgenes with fluorophores that overlapped with H2A-mCherry, such as *ubi:*RSdnM or *hsp70l:*RSN. For these analyses, the cells within the trabeculae could be separated from the ventricular outer wall using the post-image processing procedure described in the Image processing and Statistical analysis section below. Using this procedure we calculated the number of cardiomyocyte nuclei in the total ventricle and the number of cardiomyocyte nuclei within the trabeculae. The number of cardiomyocyte nuclei in the ventricular outer wall was calculated by subtracting the number of cardiomyocytes in the trabeculae from the total.

Trabeculae area was measured from a confocal slice of a ventricle containing a cytoplasmic fluorophore such as *myl7:*mCherry or *ubi:*RSdnM or *hsp70l:*RSN. Confocal slices at the level of the AV canal were analyzed. Non-trabecular tissue in these images was masked manually and then the total number of fluorescent pixels was measured using the IDL program (Research System). All images were taken at the same dimensions. Ventricle area was determined by measuring the total pixels outlined in the ventricle region using ImageJ software.

## Clonal analysis

Cardiomyocyte clones were genetically labeled by combining the *myl7:CreER* and *priZm* (*β-act2:Brainbow1.0L*)[4] transgenes and then treating with 4-hydroxytamoxifen (4-HT, Sigma). Specifically, zebrafish embryos with these transgenes were treated at 48 hpf, when the zebrafish heart consists of a single cardiomyocyte thick wall and is looped but has not initiated cardiac trabeculation, with 10 μM 4-HT or 0.1% ethanol (control) for 6 hrs at 28°C and then washed with fresh egg water several times. The dose and length of incubation of 4-HT was titrated to create small distinct clones (1-2 cells) prior to trabeculation (Extended Data Fig. 8). The total number of cardiomyocyte clones were counted from 3D reconstructions of confocal slices from hearts containing *myl7:CreER* and *priZm* transgenes. Visualization and counting of clones solely within the trabeculae were analyzed using the post-imaging processing procedure described in the Image processing and Statistical analysis section below.

## Mosaic analysis by DNA injection

To create the *hsp70l:loxp-mCherry-STOP-loxp-dnSuH-P2A-emerald* plasmid (abbreviated *hsp70l:RSdnS*), the dominant negative Suppressor of Hairless[15] (*dnSuH*) DNA construct was PCR amplified with flanking AscI and SacII restriction sites. After sequence verification, this *dnSuH* product was subcloned into the *hsp70l:loxp-mCherry-STOP-loxp-NICD-P2A-emerald*[14] construct (*hsp70l:RSN*), replacing the NICD sequence and generating the *hsp70l:loxp-mCherry-STOP-loxp-dnSuH-P2A-emerald* (*hsp70l:RSdnS*) construct for

subsequent injection studies (see below). To generate cardiomyocyte clones with constitutively-activated or inhibited Notch signaling, the I-SceI enzyme was co-injected with either the *hsp70l:RSN* plasmid (25 pg) or the *hsp70l:RSdnS* (25 pg) plasmid into 1-cell stage embryos containing *Tg(myl7:Cre; myl7:Cerulean)* or only *Tg(myl7:Cerulean)*. Embryos were then heat-shocked (as described above) at 60 hpf and imaged at 72 hpf. Cardiomyocytes containing either plasmid were detected by the co-expression of mCherry or emerald and Cerulean. The location of Notch-altered emerald$^{+}$ cardiomyocytes clones in either the ventricular outer wall or the trabeculae was determined using the method described within the Image processing and Statistical analysis section below.

## Erbb2 and BMP loss of function studies

The activity of Erbb2, a tyrosine kinase receptor, was inhibited using 1) homozygous *erbb2*$^{st50}$ mutants[18], 2) a splice morpholino targeting *erbb2* (*erbb2* MO)[10], or 3) the tyrosine kinase inhibitor AG1478 (Calbiochem). 1) *erbb2*$^{st50}$ homozygous mutant embryos were identified by the previously characterized aberrant cardiac morphology[18]. 2) The *erbb2* MO was previously characterized and shown to be specific[10]. We injected 570 pg of the *erbb2* morpholino (*erbb2* MO) or a mismatched control morpholino (control MO) into 1-cell stage embryos as previously described[10]. 3) 5 μM AG1478 (Calbiochem) or 0.1% DMSO (control) was added to embryos as previously described[10]. After incubation, embryos were washed extensively with egg water for further analysis. *erbb2* MO injections or AG1478 incubations phenocopied the *erbb2*$^{st50}$ mutant phenotype (Fig. 3, Extended Data Fig. 9).

To investigate the relationship between Notch signaling and *erbb2*, *erbb2* MO embryos or *erbb2*$^{st50}$ mutant embryos were incubated with 100 μM DAPT (Sigma) or 0.1% DMSO at 60 hpf as described above. In complementary experiments, *Tg(hsp70l:dnMAML-GFP)* embryos were injected with the *erbb2* MO and heat-shocked at 60 hpf as described above.

To inhibit BMP signaling, embryos were incubated with 30 μM of Dorsomorphin (Sigma) as previously described[41]. The efficacy of Dorsomorphin was verified by examining its effect on the BMP reporter, *Tg(BRE:d2GFP)*.

## Cell transplantation studies

Blastomere transplantation was performed at the mid-blastula stage as previously described[23]. 10-20 cells were removed from mid-blastula donor *Tg(myl7:Cerulean)* embryos and placed along the margin of either control MO or *erbb2* MO host *Tg(Tp1:d2GFP; myl7:H2A-mCherry)* embryos. Transplanted embryos in which donor cells contributed to the heart were imaged at 72 hpf. Image analysis of whether donor cells contributed to the ventricular outer wall or trabeculae and their location relative to *Tp1:*d2GFP$^{+}$ cells was assessed in single confocal slices or in 3D reconstructions using the post-imaging procedures described within the Image processing and Statistical analysis section below.

## *In Situ* Hybridization Expression Analyses

*erbb2* and *jag2b* Fluorescent *In Situ* Hybridization (FISH) studies were performed as described in the ViewRNA *in situ* hybridization 1-Plex kit protocol (Affymetrix Panomics) with the following modifications. After the initial fixation, existing fluorescence was

quenched as described for embryonic immunofluorescence above. Embryos were then subjected to protease digestion (protease QF, 1:100) at 40°C for 30 min, followed by PBST washes and re-fixation in 4% PFA at room temperature (RT) for 20 min. After additional PBST washes, hybridization was performed with *erbb2* probes (Affymetrix Panomics VF1-16871, 1:50 dilution) or *jag2b* probes (Affymetrix Panomics VF1-18462, 1:50 dilution) at 40°C overnight. Hybridized embryos were then washed in PBST and stepped through pre-labeling solutions. Embryos were then incubated with label probe-AP solution (1:1000) for 30 min at 40°C, washed again, transferred to a AP-enhancer solution and then transferred to fast red solution (1 fast red substrate tablet in 5 ml naphthol buffer) for 30 min at 40°C. After PBST washes, embryos were incubated in anti-MHC/MF20 antibody (mouse, Developmental Studies Hybridoma Bank, 1:100) or anti-GFP antibody (chicken, Aves Labs, 1:200) overnight at 4°C. Following PBST washes, embryos were incubated in anti-mouse IgG-Alexa 488 (goat, Life Technologies, 1:200) or anti-chicken IgG-Alexa 488 antibodies (goat, Life Technologies, 1:200) for 1 hr at RT. Finally, embryos were washed and mounted for imaging. PBST washing consists of 3 washes for 15 min each at RT. For *gfp* mRNA expression analysis, whole mount *in situ* hybridization studies were performed as previously described[40].

## Image processing and Statistical analysis

All images were obtained using a Nikon C2 confocal microscope and processed using Nikon NIS Elements software and ImageJ as previously described[40]. Scale bars for all images represents 25 μm. Measurements comparing the ventricular outer wall to the trabeculae were carried out with post-image processing of confocal slices. Visualization of all cardiomyocytes and clones within the ventricle (comprising both the ventricular outer wall and the trabeculae) were made using 3D reconstructions (Nikon NIS Elements) of confocal slices. However to visualize only the trabeculae, cardiomyocytes within the ventricular outer wall in individual confocal slices were identified by their outer location and orientation and then masked manually. 3D reconstructions with these masked confocal slices then allowed the visualization and measurement of trabeculae alone. Measurements for the ventricular outer wall alone were calculated by subtracting the measurements of the trabeculae from the total ventricular cardiomyocytes. No statistical methods were used to predetermine sample size. Animals were assigned to experimental groups using simple randomization, without investigator blinding. Unpaired two-tailed Student's *t*-tests or Fisher's exact tests were used to determine statistical significance. A p value $< 0.05$ was considered to be statistically significant, as indicated by *. Error bars represent standard error means (s.e.m.).

## Extended Data

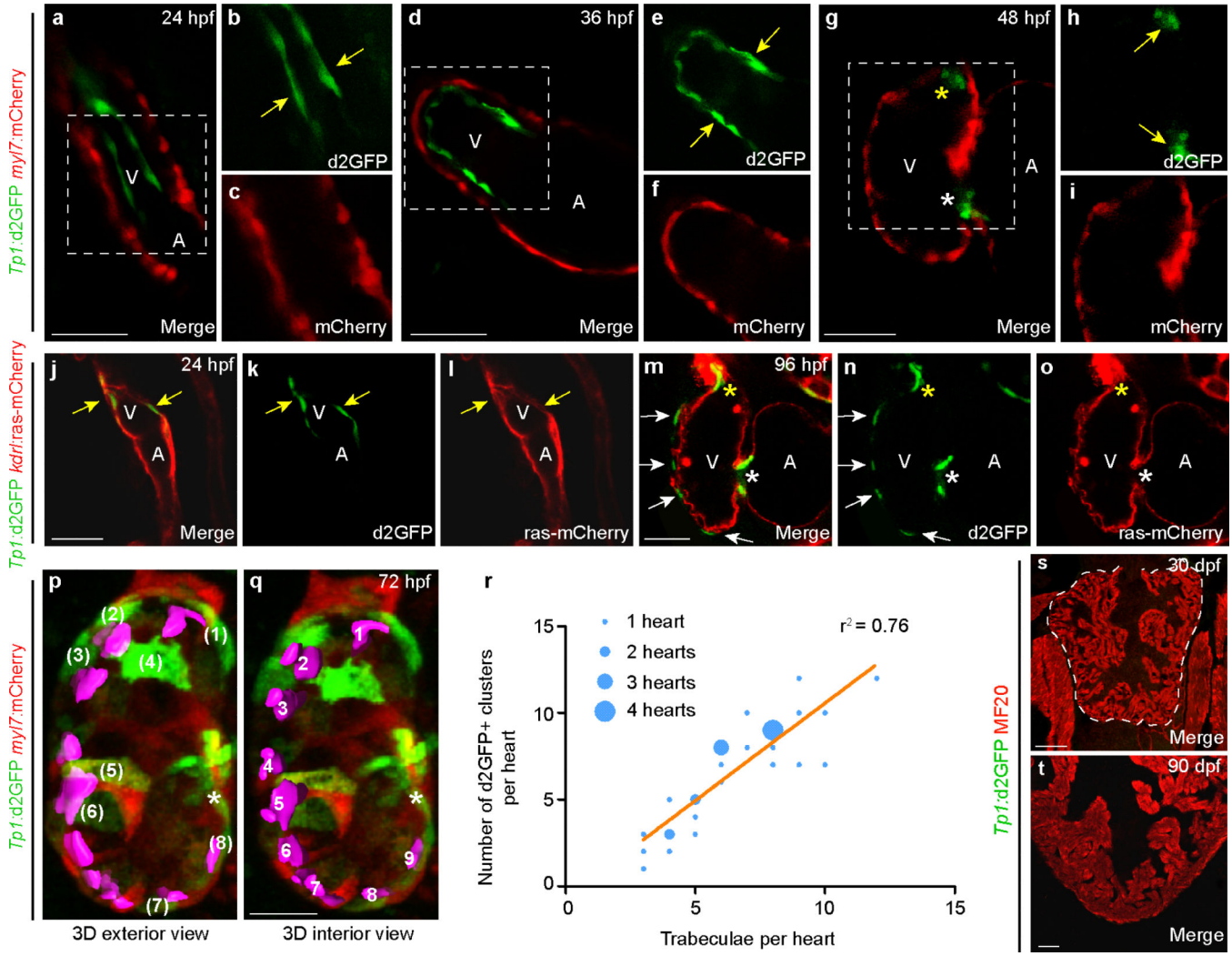


**Extended Data Figure 1. Notch signaling is dynamically activated in the endocardium and myocardium during heart development**

**a-f**, Confocal slices of *Tg(Tp1:d2GFP; myl7:mCherry)* hearts reveal that Notch signaling is in the ventricular endocardium (yellow arrows) but not in the myocardium at 24 hpf (n = 11) and 36 hpf (n = 8), **g-i,** but becomes restricted to the AV and OFT endocardium by 48 hpf (n = 12). **j-o**, *Tg(Tp1:d2GFP; kdrl:ras-mCherry)* confocal imaging confirms that *Tp1:*d2GFP is expressed in the ventricular endocardium at (**j-l**) 24 hpf (n = 8) but becomes localized to the AV or OFT endocardium as well as non-endocardial cells in the outer ventricular myocardial wall (white arrows) by (**m-o**) 96 hpf (n = 10). **p**, **q**, 3D confocal reconstructions of the (**p**) exterior and (**q**) interior regions of 72 hpf *Tg(Tp1:d2GFP; myl7:mCherry)* hearts reveal that Notch-activated *Tp1:*d2GFP$^{+}$ cells are present in cardiomyocyte clusters (green, numbers in parentheses) and excluded from nascent cardiac trabeculae (pseudo-color magenta, numbers). **r**, Graph shows that the number of cardiac trabeculae (x-axis) and *Tp1:*d2GFP$^{+}$ cardiomyocyte clusters (y-axis) are similar within the ventricle (n = 30) at 72 hpf. Size of dots indicates the number of embryos with a particular number of trabeculae and

*Tp1:*d2GFP$^{+}$ clusters. Line represents a linear regression fitted to the data. **s**, **t**, Myocardial anti-MHC/MF20 immunostaining of *Tg(Tp1:d2GFP)* hearts reveals a loss of myocardial *Tp1:*d2GFP Notch reporter signal at 30 and 90 dpf hearts (n = 5 hearts per stage). White arrows – likely *Tp1:*d2GFP$^{+}$ cardiomyocytes, yellow arrows – *Tp1:*d2GFP$^{+}$ endocardial cells. White and yellow asterisks – AV and OFT. Dashed line in **s** outlines ventricle. V–ventricle; A – atrium. Scale bar 25 μm.

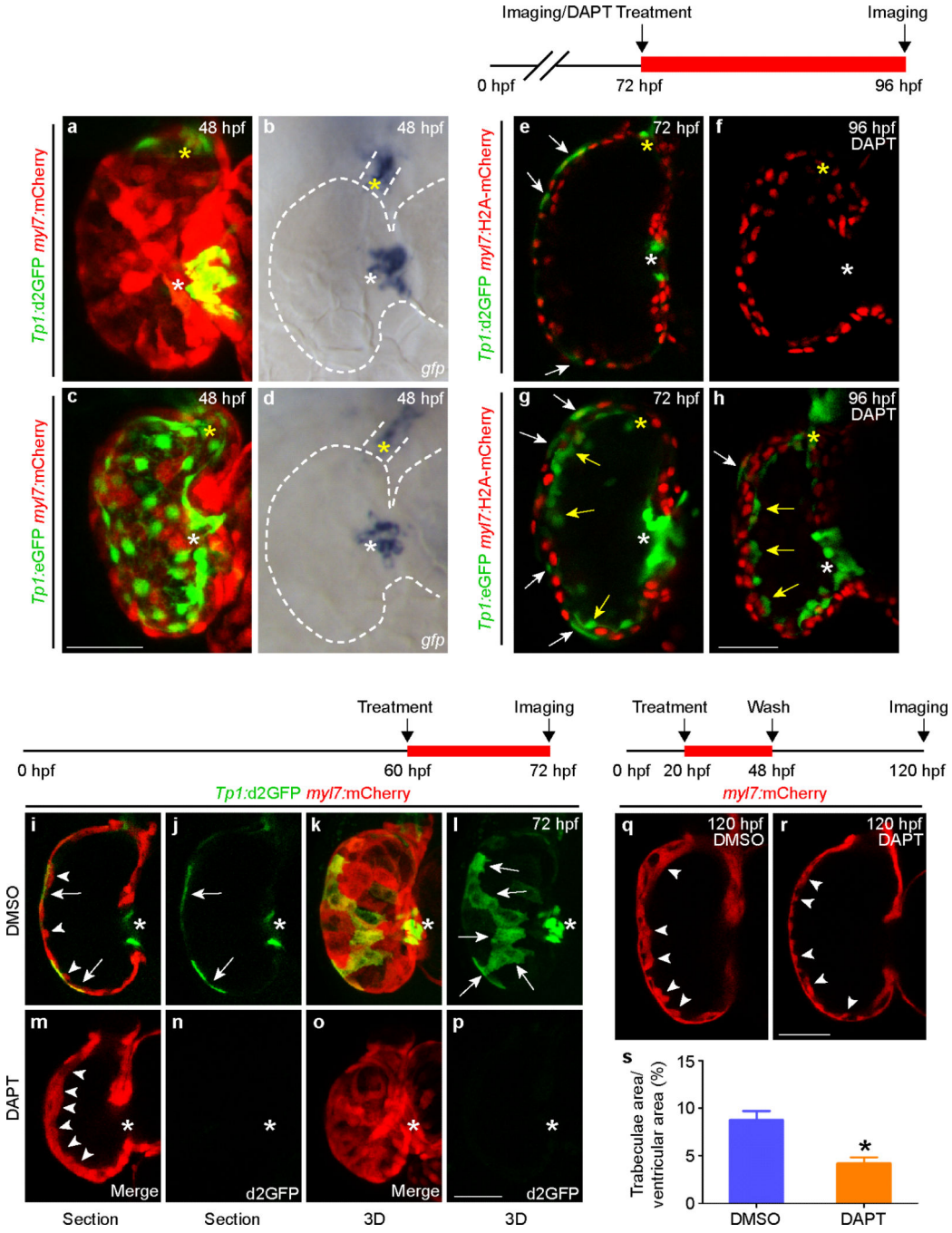

**Extended Data Figure 2. DAPT treatment validates that the Notch reporter *Tp1:*d2GFP monitors dynamic Notch signaling more closely than *Tp1:*eGFP, and reveals opposing roles of Notch signaling on trabeculation at different developmental stages**

**a-d**, At 48hpf, (**a**) *Tp1*:d2GFP expression is restricted to the AV and OFT endocardium (n = 8/8 embryos) whereas (**c**) *Tp1*:eGFP is expressed in the ventricular, AV and OFT endocardium (n = 6/6). However, *gfp* mRNA is primarily expressed in the AV and OFT regions in both (**b**) *Tg(Tp1:d2GFP; myl7:mCherry)* (n = 10/10) and (**d**) *Tg(Tp1:eGFP; myl7:mCherry)* embryos (n = 5/5), revealing that *Tp1*:d2GFP expression most closely matches Notch reporter activity. **e-h**, After 24 hour DAPT treatments of (**e, f**) *Tg(Tp1:d2GFP; myl7:H2A-mCherry)* and (**g, h**) *Tg(Tp1:eGFP; myl7:H2A-mCherry)* embryos at 72 hpf, (**f**) *Tp1:*d2GFP is more diminished throughout the heart at 96 hpf (n = 8/10) compared to (**h**) *Tp1:*eGFP (n = 6/7), confirming *Tp1*:d2GFP signal more faithfully recapitulates Notch signaling dynamics. **m-p**, *Tg(Tp1:d2GFP; myl7:mCherry)* hearts DAPT-treated from 60-72 hpf exhibit increased trabeculation (white arrowheads) and diminished *Tp1:*d2GFP Notch reporter activity (n = 12/16) compared to (**i-l**) DMSO-treated hearts (n = 0/20). However, (**r**) *Tg(myl7:mCherry)* hearts DAPT-treated from 20 to 48 hpf exhibit reduced trabeculae at 120 hpf (n = 12/15) when compared to (**q**) DMSO treated hearts (n = 0/20). **s**, Graph represents trabeculae/total ventricular area in embryos treated with DMSO or DAPT in **q** and **r**. White and yellow arrows – myocardial and endocardial Notch reporter activity. White arrowheads – trabeculae. White and yellow asterisks – AV and OFT. Scale bar 25 μm. Mean +/− s.e.m. *$p < 0.05$ by Student's *t*-test.

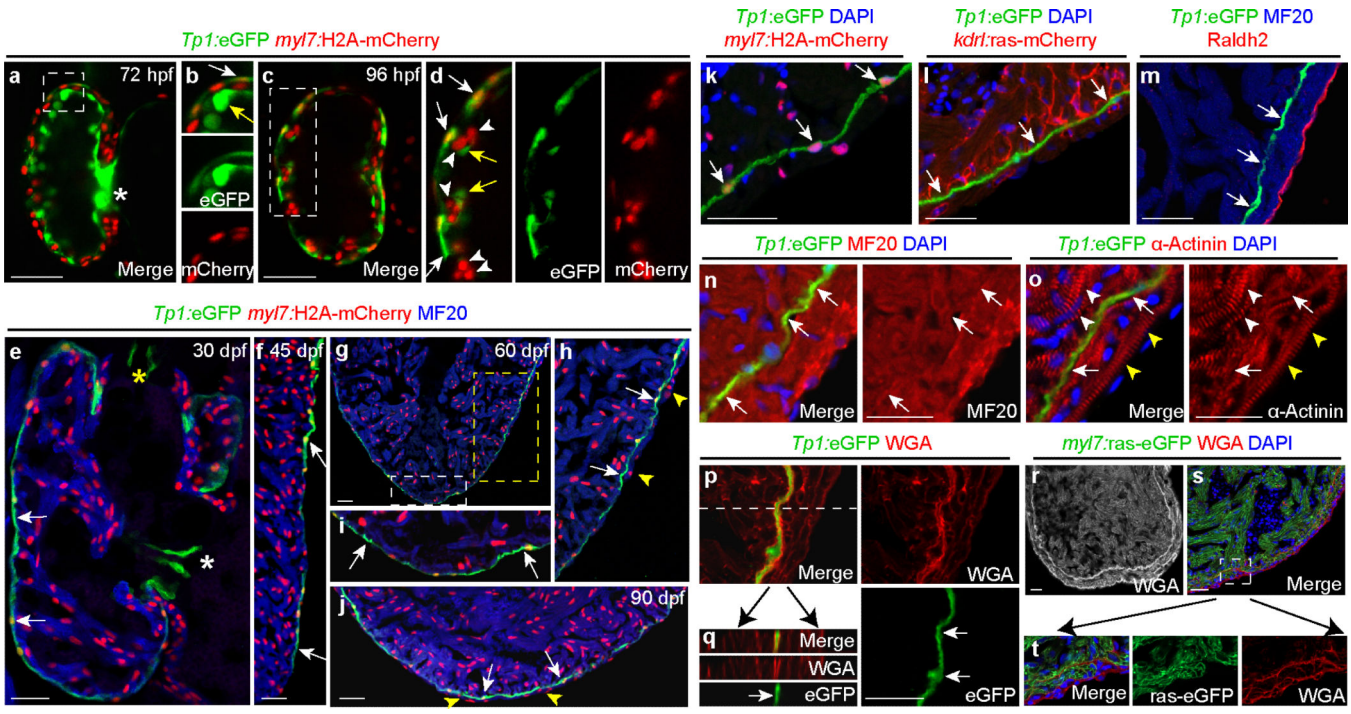


**Extended Data Figure 3. *Tp1*:eGFP labels the ventricular outer wall during early cardiac development, which becomes the distinctive ventricular primordial myocardium in adults**

Using the *Tp1:*eGFP Notch reporter which exhibits greater fluorescence perdurance than *Tp1:*d2GFP, we performed limited fate mapping of Notch activated cardiac cells during ventricular morphogenesis. **a-d**, *Tp1:*eGFP is expressed not only in ventricular

cardiomyocytes (red nuclei, white arrows) at 72 hpf but also throughout the ventricular endocardium due to eGFP perdurance (yellow arrows) (n = 12). **c, d**, Although diminishing in the ventricular endocardium (yellow arrows) at 96 hpf (n = 14), *Tp1:*eGFP expands in the outer ventricular myocardial wall (white arrows), yet is notably absent from myocardial trabeculae (white arrowheads). **e, f**, By 30 and 45 dpf (n = 6, n = 5), *Tp1:*eGFP remains in the peripheral ventricular (primordial) myocardial layer, which is one-cardiomyocyte thick (*myl7:*H2A-mCherry$^{+}$/red and MF20$^{+}$/blue), but is reduced in the ventricular but not the AV or OFT endocardium. **g-i**, At 60 dpf (n = 5), (**h**) new cardiomyocytes (cortical layer, yellow arrowheads) form over the *Tp1:*eGFP$^{+}$ primordial myocardium (white arrows) at the ventricular myocardial base (yellow box in **g**) and extends toward the apex where (**i**) *Tp1:*eGFP$^{+}$ cardiomyocytes (white arrows) still remain the outer most layer of the ventricular myocardium (white box in **g**). **j**, However, by 90 dpf (n = 5), this new cortical myocardial layer (yellow arrowheads) spreads over the apical *Tp1:*eGFP$^{+}$ ventricular primordial myocardium (white arrows). **k-m**, In adult hearts (90 dpf), *Tp1:*eGFP is primarily found in the (**k**, n = 5) *myl7:*H2A-mCherry$^{+}$ primordial myocardium but not in the (**l**, n = 5) endocardium marked by *kdrl:*ras-mCherry, nor (**m**, n = 3) epicardium marked by Raldh2 localization. **n-t**, Adult hearts (6 months) were further examined to assess the cellular attributes of the primordial layer. **n**, Anti-MHC/MF20 immunostaining confirms that *Tp1:*eGFP$^{+}$ cardiac cells are myocardial (n = 5). **o**, Anti-α–actinin immunostaining reveals that trabecular (white arrowheads) and cortical (yellow arrowheads) cardiomyocytes display organized sarcomeric structures but the *Tp1:*eGFP$^{+}$ primordial cardiomyocytes (arrows) do not (n = 7). **p-t**, Wheat germ agglutinin (WGA) staining shows that (**p, q**) the *Tp1:*eGFP$^{+}$ primordial myocardial layer is surrounded by extensive extracellular matrix (n = 5) and that (**r-t**) *Tg(myl7:ras-eGFP)* primordial cardiomyocytes display a thin cellular morphology compared to other ventricular cardiomyocytes (n = 10). **q** is a X-Z reconstruction of confocal stacks from *Tp1:*eGFP and WGA stainings at the dashed line shown in **p. b, d, h-i, t** are magnifications of the boxed area in **a, c, g, s,** respectively. White and yellow arrows – myocardial and endocardial *Tp1:*eGFP. White and yellow arrowheads – trabeculae and cortical layer. White and yellow asterisks – AV and OFT. Scale bar 25 μm.

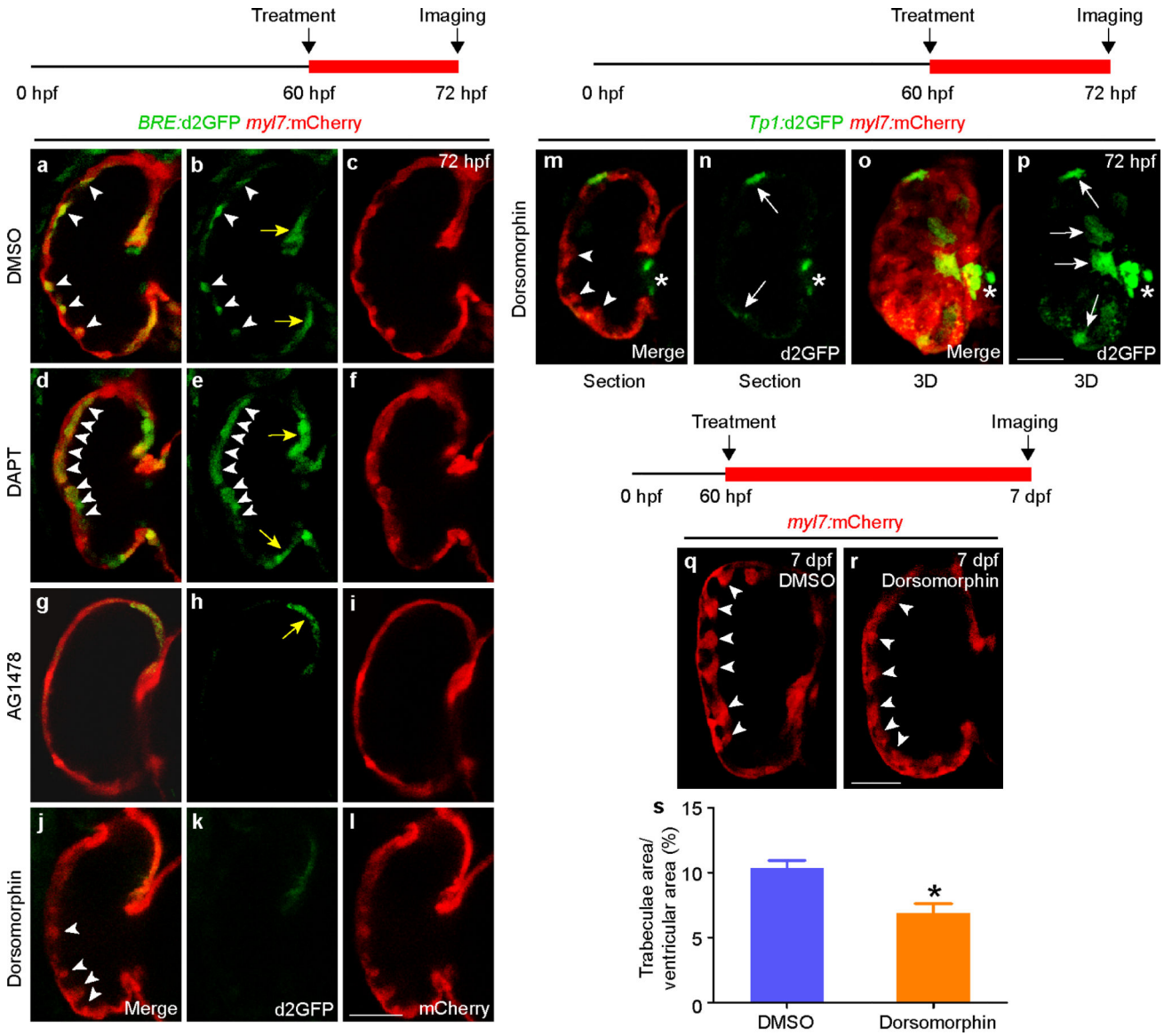


**Extended Data Figure 4. Bmp signaling, which marks trabeculae, is required for expanding but not initiating trabeculae formation and has no effect on myocardial Notch activity**

**a-l**, *Tg(BRE:d2GFP; myl7:mCherry)* hearts were treated with (**a-c**) DMSO, (**d-f**) DAPT, (**g-i**) AG1478 or (**j-l**) Dorsomorphin at 60 hpf and imaged at 72 hpf. **a-c**, DMSO treated hearts express the *BRE:*d2GFP BMP reporter in trabeculae (arrowheads) and in the AV myocardium (yellow arrows, n = 11/11 embryos). **d-f**, DAPT treated hearts exhibit increased trabeculation and *BRE:*d2GFP expression in these forming trabeculae (arrowheads, n = 9/12). **g-i**, AG1478 treated hearts fail to form trabeculae (n = 9/10) and only express the *BRE:*d2GFP BMP reporter in the AV myocardium (yellow arrow). **j-l**, Dorsomorphin treated hearts form cardiac trabeculae (arrowheads) but fail to express the *BRE:*d2GFP BMP reporter in both cardiac trabeculae and the AV myocardium (n = 10/12). **m-p**, Treating *Tg(Tp1:d2GFP; myl7:mCherry)* embryos with Dorsomorphin from 60-72 hpf did not affect the initiation of trabeculae (arrowheads) nor the activation of myocardial Notch signaling (white arrows, n = 13/16) compared to treating with DMSO (see Extended Data Fig. 2i-l). **q,**

**r**, Although *Tg(myl7:mCherry)* hearts treated with (**q**) DMSO or (**r**) Dorsomorphin from 60 hpf to 7 dpf form similar numbers of trabeculae (arrowheads), Dorsomorphin-treated hearts display trabeculae that are stunted/reduced in size (n = 12/15) when compared to DMSO-treated control hearts (n = 0/15). **s**, Graph reveals a significant reduction in the trabecular/ventricular area ratio in Dorsmorphin-treated fish compared to DMSO-treated controls. Arrowheads – trabeculae, yellow arrows – AV myocardium, white arrows – *Tp1*:d2GFP$^{+}$ myocardium. White asterisks – AV. Mean +/− s.e.m. *$p < 0.05$ by Student's *t*-test. Scale bar 25 μm.

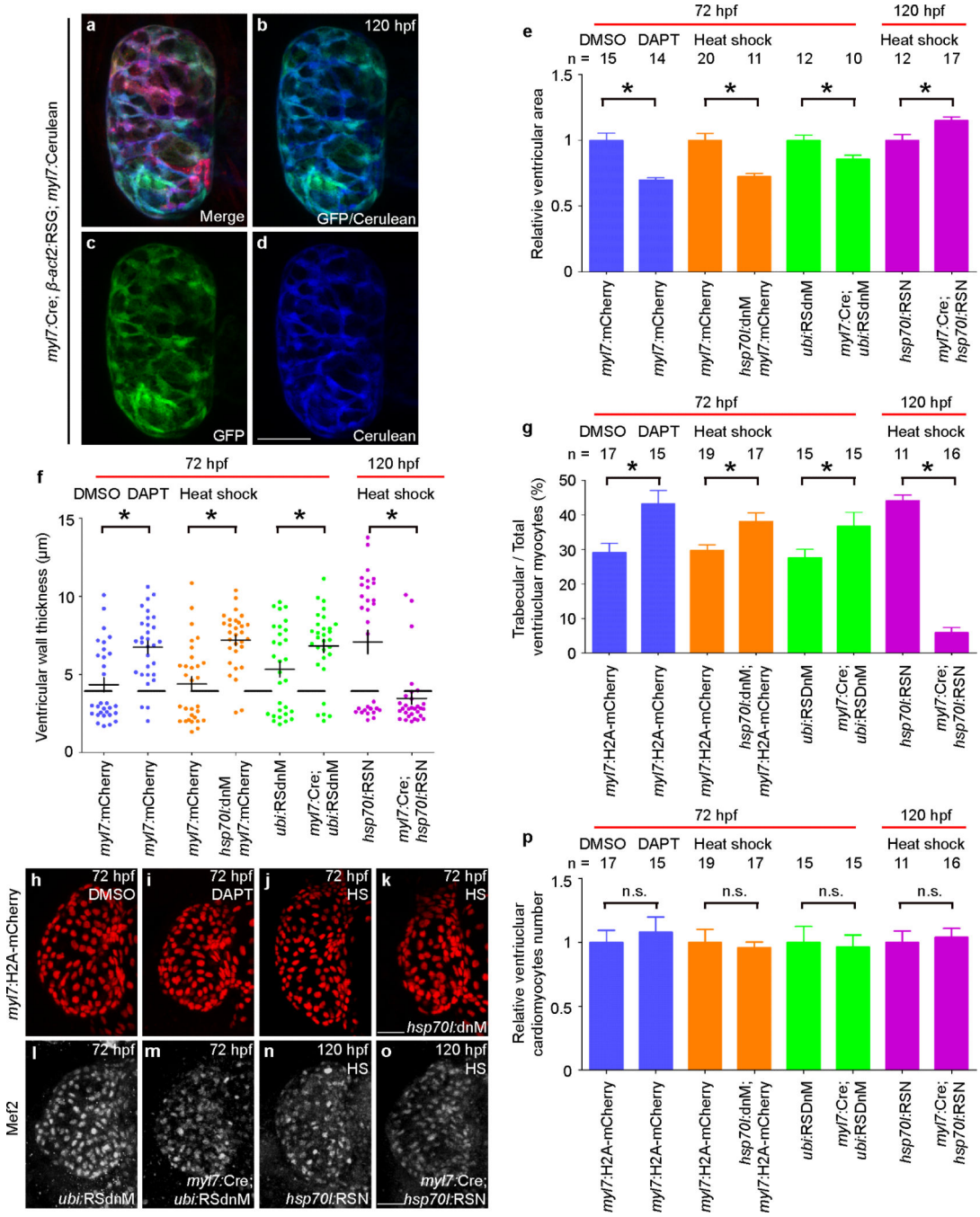


**Extended Data Figure 5. Altering myocardial Notch signaling affects ventricular size and wall thickness but not total number of ventricular cardiomyocytes**

**a-d**, The *Tg(myl7:Cre)* transgenic line used to specifically perturb Notch signaling in the myocardium was validated by confirming that Cre expression is restricted to the myocardium. *myl7:*Cre activity as visualized by (**c**) GFP expression from the switch line, *β-act2:*RSG, exclusively overlaps with (**b**, **d**) *myl7:*Cerulean expression at 120 hpf (n = 10 embryos). Quantitative analyses of (**e**) ventricular size and (**f**) wall thickness performed on confocal images from Figure 2**a-h** reveal that myocardial Notch signaling restricts

ventricular size while promoting ventricular wall thickness. **e**, Ventricular size measurements were normalized to respective controls for each condition. **f**, Individual measurements (dots) of myocardial thickness were taken across the outer curvature of the ventricle (n = 30 measurements, 6 measurements were taken per embryo, 5 embryos per condition). Dashed line represents the ventricular wall thickness that distinguishes trabeculated myocardial thickness from ventricular outer wall myocardial thickness in control hearts. Crosses denote mean and s.e.m. **g-p**, Quantitative analysis of (**g**) trabecular cardiomyocytes and (**p**) total ventricular cardiomyocytes was calculated by counting myocardial nuclei labeled with *myl7:*H2A-mCherry or anti-Mef2 immunostaining using embryos from Figure 2**i-p** for (**g**), or from 3D reconstructions in (**h-o**) for (**p**). In (**g**), trabecular/total ventricular cardiomyocytes was used to calculate the percentage of trabecular cardiomyocytes for each condition. In (**p**), total ventricular cardiomyocytes were normalized to respective controls for each condition. n – number of embryos analyzed per condition. Mean +/− s.e.m. $*p < 0.05$ by Student's *t*-test. n.s. – not significant. Scale bar 25 μm.

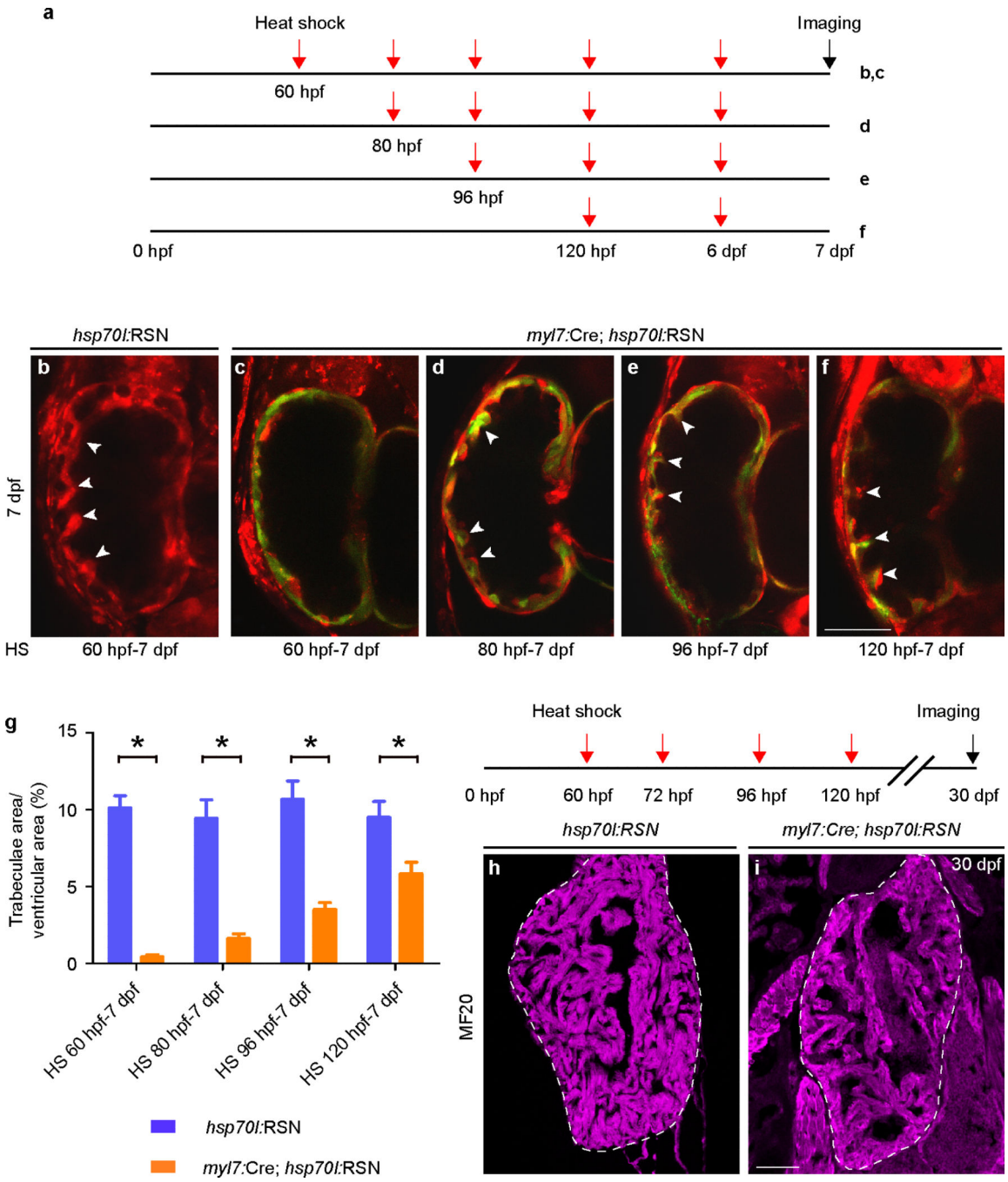


**Extended Data Figure 6. Myocardial Notch activation can inhibit the formation and expansion of cardiac trabeculae at various cardiac developmental stages**

**a-g**, *Tg(myl7:Cre; hsp70l:RSN)* and *Tg(hsp70l:RSN)* (control) embryos were heat-shocked (HS) during various developmental time windows as indicated and imaged at 7 dpf to assess the effects of constitutive myocardial Notch signaling on cardiac trabeculae formation. **a**, Red arrows in schematic indicate the time points in which embryos in the corresponding panels were heat-shocked. **b**, Control *Tg(hsp70l:RSN)* embryos heat-shocked from 60 hpf to 7 dpf ubiquitously express mCherry but do not overexpress myocardial NICD. They form

cardiac trabeculae (arrowheads) similar to wild-type embryos (control, n = 14/15). **c**, However, *Tg(myl7:Cre; hsp70l:RSN)* embryos heat-shocked from 60 hpf to 7 dpf overexpress NICD-P2A-Emerald throughout the myocardium and fail to form cardiac trabecuale (n = 9/12). Although *Tg(myl7:Cre; hsp70l:RSN)* embryos heat-shocked at (**d**) 80 hpf – 7 dpf, (**e**) 96 hpf – 7 dpf, and (**f**) 120 hpf – 7 dpf form trabeculae, these embryos exhibit stunted/smaller trabeculae after heat-shocking (n = 9/10, 10/14, 12/16, respectively). **g**, Graph of trabeculae/total ventricular area of heat-shocked embryos from **b-f**, shows that myocardial Notch over-activation inhibits the progression of cardiac trabeculae formation. **h**, **i**, Although heat-shocking *Tg(myl7:Cre; hsp70l:RSN)* from 60-120 hpf initially inhibits trabeculae formation, (**i**) the ventricular myocardium (detected by anti-MHC/MF20 immunostaining – magenta) can still form trabeculae albeit at reduced numbers (n = 4/5) by 30 dpf after stopping NICD overexpression when compared to (**h**) heat-shocked *Tg(hsp70l:RSN)* hearts (control, n = 0/8). HS – heat-shock. White arrowheads – trabeculae. Scale bar 25 μm. Mean +/− s.e.m. *$p < 0.05$ by Student's *t*-test.

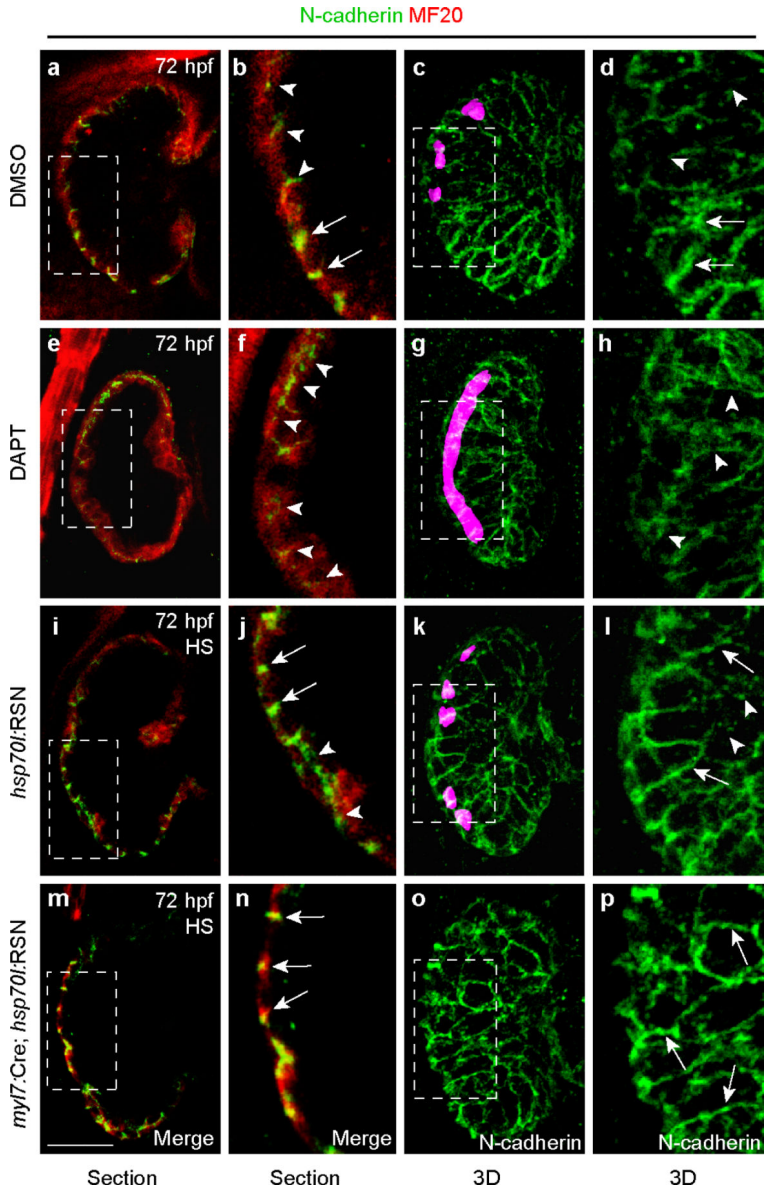


**Extended Data Figure 7. Notch signaling regulates cardiomyocyte cell junctions during cardiac trabeculae formation**

**a-d**, In DMSO treated (control) 72 hpf wild-type hearts, N-cadherin is localized at cell junctions of cardiomyocytes within the ventricular outer wall (arrows) but redistributes away from these cell-cell contacts in cardiomyocytes that extend into the lumen to form trabeculae (arrowheads) (n = 12/12). **e-h**, Notch inhibition by DAPT treatment promotes N-cadherin redistribution and results in increased trabeculation (n = 8/11). **m-p**, Conversely, myocardial Notch activation by heat shocking (HS) *Tg(myl7:Cre; hsp70l:RSN)* leads to diminished N-cadherin redistribution and reduced trabeculation (n = 7/10) compared to (**i-l**) heat-shocked *Tg(hsp70l:RSN)* control hearts (n = 0/10). Nascent cardiac trabeculae were pseudo-colored magenta in (**c, g, k**). **b, d, f, h, j, l, n, p**, Insets are magnifications of **a, c, e, g, i, k, m, o** boxed areas, respectively. Arrowheads – N-cadherin redistributed from cell-cell contacts, arrows – N-cadherin at cell-cell contacts within outer wall. Scale bar 25 μm.

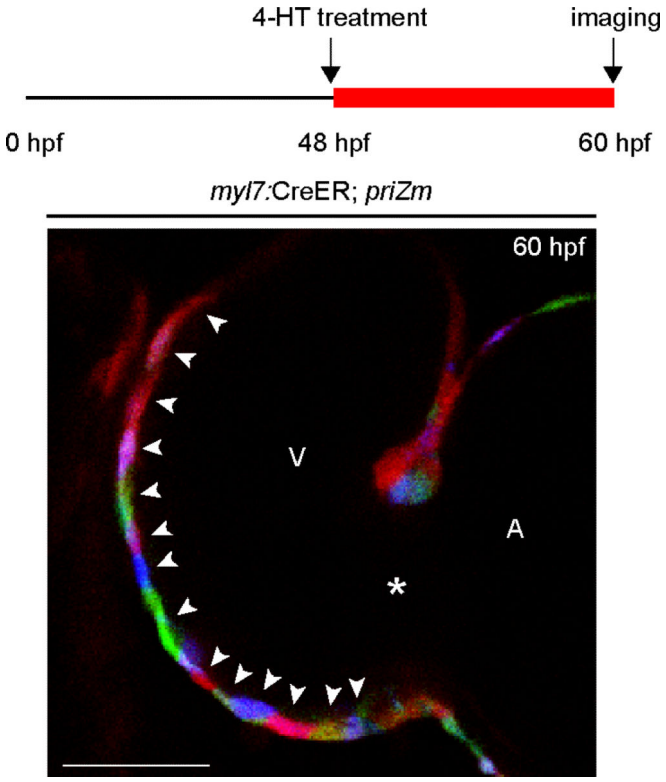


**Extended Data Figure 8. Tamoxifen treatment of *Tg(myl7:CreER; priZm)* embryos at 48 hpf labels adjacent individual cardiomyocytes with combinations of distinct fluorescent colors**

*Tg(myl7:CreER; priZm)* embryos were treated with 4-HT at 48 hpf and confocal imaged at 60 hpf prior to the initiation of cardiomyocytes forming trabeculae. Individual cardiomyocytes (arrowheads) are labeled with distinct combinations of fluorescent proteins allowing for tracking of specific cardiomyocyte clones (n = 6). White arrowheads – cardiomyocytes. V – ventricle, A – atrium. White asterisk – AV. Scale bar 25 μm.

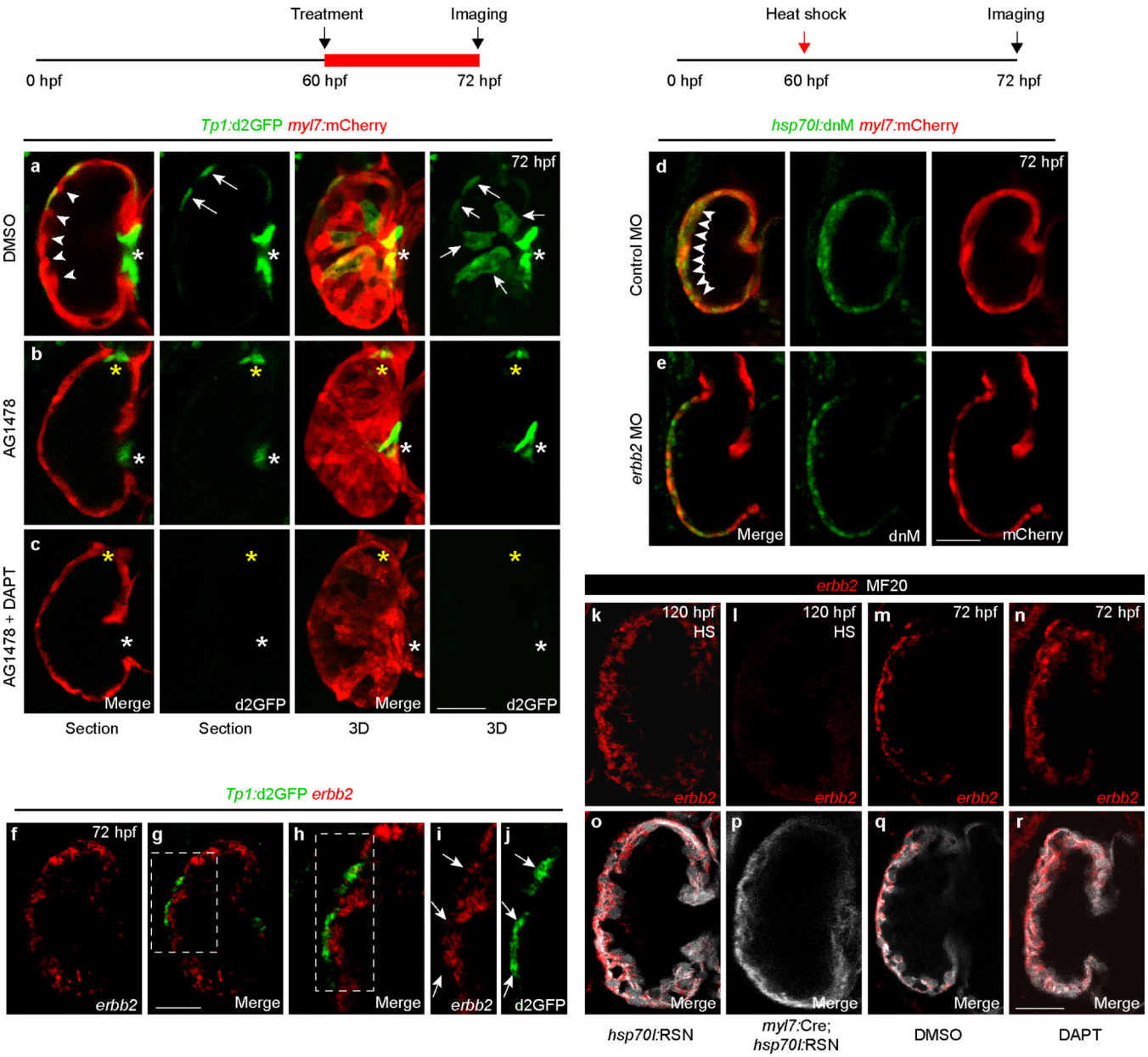


**Extended Data Figure 9. Notch and Erbb2 signaling pathways form a feedback loop during cardiac trabeculation**

**a-c**, Compared to (**a**) DMSO-treated *Tg(Tp1:d2GFP; myl7:mCherry)* (controls) embryos, (**b**) inhibiting Erbb2 function with AG1478 from 60-72 hpf blocks trabeculation and myocardial Notch signaling (n = 14/17), confirming *erbb2* MO and mutant phenotypes. **c**, However, Notch inhibition using DAPT cannot reverse the AG1478/Erbb2 inhibition effect on trabeculae formation (n = 11/12). **d, e**, Consistent with these results, (**d**) control MO-injected *Tg(hsp70l:dnM; myl7:mCherry)* embryos expressing heat-shock induced dnMAML from 60-72 hpf display increased trabeculation (arrowheads, n = 9/11); (**e**) however, *erbb2* MO-injected embryos expressing heat-shock induced dnMAML fail to display trabeculae (n = 9/12) as similarly observed in *erbb2* MO-injected embryos alone (Fig. 3). **f-j**, *erbb2*

fluorescent *in situ* hybridization and GFP co-immunostaining performed on 72 hpf *Tg(Tp1:d2GFP)* hearts reveal that *erbb2* is expressed in an intermittent pattern across the ventricular wall and is specifically diminished in *Tp1*:d2GFP$^{+}$ cells (arrows) (n = 6/6). **l, p**, Heat-shocked (HS) *Tg(myl7:Cre; hsp70l:RSN)* hearts, which exhibit constitutively activated myocardial Notch signaling (NICD) from 60-120 hpf, minimally express *erbb2* in the myocardium (n = 8/11) compared to (**k, o**) heat-shocked *Tg(hsp70l:RSN)* control hearts (n = 0/20) at 120 hpf. Compared to (**m, q**) DMSO treated control hearts (n = 0/10), (**n, r**) Notch-inhibited hearts by DAPT treatment from 60-72 hpf exhibit increased myocardial *erbb2* expression as well as more trabeculae at 72 hpf (n = 8/10), supporting that Notch signaling inhibits *erbb2* expression. **h, i-j** are magnifications of boxed areas in **g, h**. Arrowheads – trabeculae, arrows – *Tp1*:d2GFP$^{+}$ cardiomyocytes. White and yellow asterisks – AV and OFT. Scale bar 25 μm.

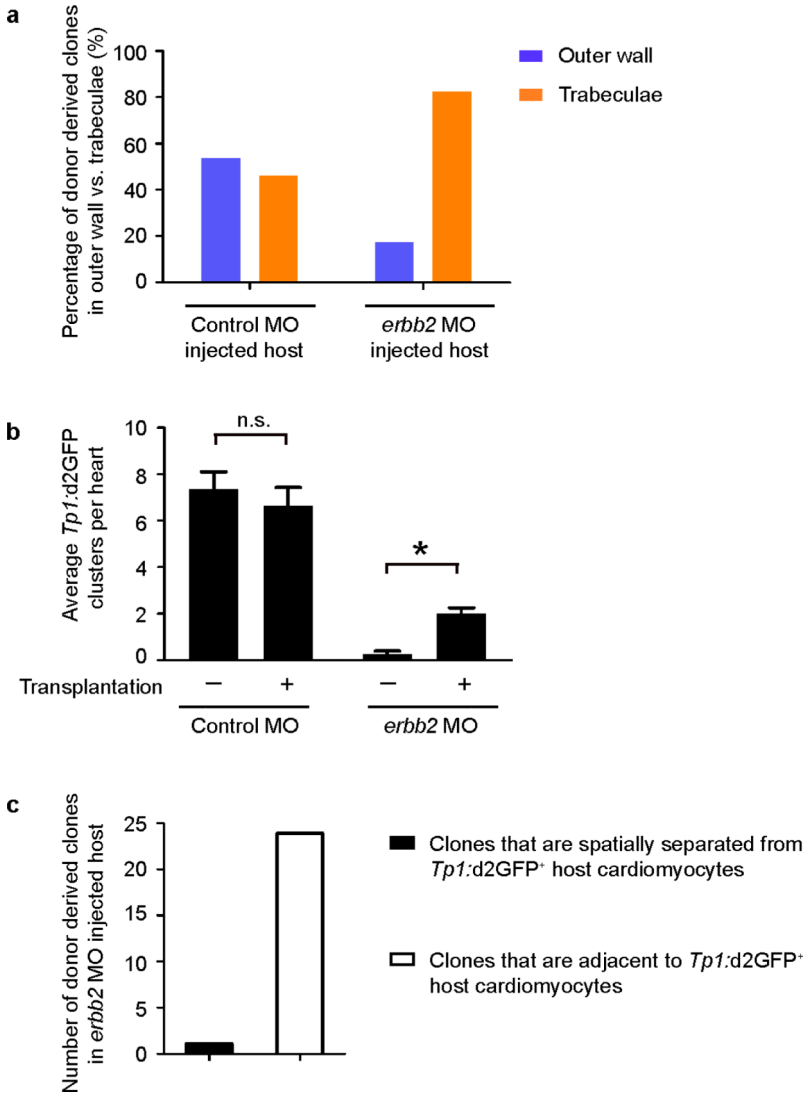


**Extended Data Figure 10. Transplanted wild-type cardiomyocytes non-cell-autonomously activate Notch signaling in *erbb2* morphant host cardiomyocytes**

**a**, Based on mosaic embryo studies from Figure 3**f-i**, wild-type donor cardiomyocytes contribute equally to the outer ventricular wall (14/26 clones) or the trabeculae (12/26 clones) when transplanted into control MO host embryos (n = 12 embryos). However, when wild-type donor cells are transplanted into *erbb2* MO host embryos (n = 10 embryos), they contribute more to the trabecular layer (19/23 clones) than to the ventricular outer wall (4/23 clones, Fisher's exact test $p < 0.05$). **b**, Based on mosaic embryo studies from Figure 3**f-i**, transplanting wild-type donor cells increases the number of *erbb2* MO host cardiomyocytes expressing *Tp1:*d2GFP (n = 10 embryos) compared to non-transplanted *erbb2* MO embryos (n = 16 embryos), but had no effect on the number of control MO host cells expressing *Tp1:*d2GFP (n = 12 embryos) compared to non-transplanted controls (n = 11 embryos). **c**, Quantitative data for Figure 3**f-i** reveals that transplanted wild-type donor cardiomyocytes are primarily adjacent to host *Tp1:*d2GFP$^{+}$ cardiomyocytes in *erbb2* MO hearts (n = 10 embryos). Mean +/− s.e.m. *$p < 0.05$ by Student's *t*-test. n.s. – not significant.

## Acknowledgements

We thank N. Tedeschi for fish care; B. Le for experimental assistance; S. Evans, D. Yelon and Chi lab members for comments on the manuscript; N. Ninov and D. Stainier for plasmids; B. Link for the d2GFP BMP and d2GFP Notch reporter lines; N. Lawson for the eGFP Notch reporter line; B. Appel for the myocardial Cerulean line; K.Poss for the myocardial CreER and Brainbow/priZm lines and W. Talbot for the *erbb2* mutant. This work was supported in part by grants from American Heart Association (14POST20380738) to L.Z.; the March of Dimes (#1-FY14-327) to R.A.M.; the NIH/NHLBI (5R01HL127067) to C.G.B. and C.E.B.; the NIH to N.C.C.

## References

1. Fahed AC, Gelb BD, Seidman JG, Seidman CE. Genetics of congenital heart disease: the glass half empty. Circ Res. 2013; 112:707–720. [PubMed: 23410880]
2. Zemrak F, et al. The relationship of left ventricular trabeculation to ventricular function and structure over a 9.5-year follow-up: the MESA study. Journal of the American College of Cardiology. 2014; 64:1971–1980. [PubMed: 25440091]
3. Grego-Bessa J, et al. Notch signaling is essential for ventricular chamber development. Dev Cell. 2007; 12:415–429. [PubMed: 17336907]
4. Gupta V, Poss KD. Clonally dominant cardiomyocytes direct heart morphogenesis. Nature. 2012; 484:479–484. [PubMed: 22538609]
5. Staudt DW, et al. High-resolution imaging of cardiomyocyte behavior reveals two distinct steps in ventricular trabeculation. Development. 2014; 141:585–593. [PubMed: 24401373]
6. Ghabrial AS, Krasnow MA. Social interactions among epithelial cells during tracheal branching morphogenesis. Nature. 2006; 441:746–749. [PubMed: 16760977]
7. Siekmann AF, Lawson ND. Notch signalling limits angiogenic cell behaviour in developing zebrafish arteries. Nature. 2007; 445:781–784. [PubMed: 17259972]
8. Clark BS, et al. Loss of Llgl1 in retinal neuroepithelia reveals links between apical domain size, Notch activity and neurogenesis. Development. 2012; 139:1599–1610. [PubMed: 22492354]
9. Samsa LA, et al. Cardiac contraction activates endocardial Notch signaling to modulate chamber maturation in zebrafish. Development. 2015; 142:4080–4091. [PubMed: 26628092]
10. Liu J, et al. A dual role for ErbB2 signaling in cardiac trabeculation. Development. 2010; 137:3867–3875. [PubMed: 20978078]
11. Ong LL, Kim N, Mima T, Cohen-Gould L, Mikawa T. Trabecular myocytes of the embryonic heart require N-cadherin for migratory unit identity. Dev Biol. 1998; 193:1–9. [PubMed: 9466883]
12. Parsons MJ, et al. Notch-responsive cells initiate the secondary transition in larval zebrafish pancreas. Mech Dev. 2009; 126:898–912. [PubMed: 19595765]
13. Zhao L, et al. Notch signaling regulates cardiomyocyte proliferation during zebrafish heart regeneration. Proc Natl Acad Sci U S A. 2014; 111:1403–1408. [PubMed: 24474765]

14. Anderson RM, et al. Hepatocyte growth factor signaling in intrapancreatic ductal cells drives pancreatic morphogenesis. PLoS Genet. 2013; 9:e1003650. [PubMed: 23935514]
15. Ninov N, Borius M, Stainier DY. Different levels of Notch signaling regulate quiescence, renewal and differentiation in pancreatic endocrine progenitors. Development. 2012; 139:1557–1567. [PubMed: 22492351]
16. Mathews ES, et al. Mutation of 3-hydroxy-3-methylglutaryl CoA synthase I reveals requirements for isoprenoid and cholesterol synthesis in oligodendrocyte migration arrest, axon wrapping, and myelin gene expression. J Neurosci. 2014; 34:3402–3412. [PubMed: 24573296]
17. Peshkovsky C, Totong R, Yelon D. Dependence of cardiac trabeculation on neuregulin signaling and blood flow in zebrafish. Dev Dyn. 2011; 240:446–456. [PubMed: 21246662]
18. Lyons DA, et al. erbb3 and erbb2 are essential for schwann cell migration and myelination in zebrafish. Curr Biol. 2005; 15:513–524. [PubMed: 15797019]
19. Collery RF, Link BA. Dynamic smad-mediated BMP signaling revealed through transgenic zebrafish. Dev Dyn. 2011; 240:712–722. [PubMed: 21337469]
20. Chen H, et al. BMP10 is essential for maintaining cardiac growth during murine cardiogenesis. Development. 2004; 131:2219–2231. [PubMed: 15073151]
21. Sternberg PW. Lateral inhibition during vulval induction in Caenorhabditis elegans. Nature. 1988; 335:551–554. [PubMed: 3419532]
22. Heitzler P, Simpson P. The choice of cell fate in the epidermis of Drosophila. Cell. 1991; 64:1083–1092. [PubMed: 2004417]
23. Schumacher JA, Bloomekatz J, Garavito-Aguilar ZV, Yelon D. tal1 Regulates the formation of intercellular junctions and the maintenance of identity in the endocardium. Dev Biol. 2013; 383:214–226. [PubMed: 24075907]
24. Rentschler S, et al. Notch signaling regulates murine atrioventricular conduction and the formation of accessory pathways. J Clin Invest. 2011; 121:525–533. [PubMed: 21266778]
25. Zhao C, et al. Numb family proteins are essential for cardiac morphogenesis and progenitor differentiation. Development. 2014; 141:281–295. [PubMed: 24335256]
26. Yang J, et al. Inhibition of Notch2 by Numb/Numblike controls myocardial compaction in the heart. Cardiovasc Res. 2012; 96:276–285. [PubMed: 22865640]
27. Leimeister C, Externbrink A, Klamt B, Gessler M. Hey genes: a novel subfamily of hairy- and Enhancer of split related genes specifically expressed during mouse embryogenesis. Mech Dev. 1999; 85:173–177. [PubMed: 10415358]
28. Li L, et al. Alagille syndrome is caused by mutations in human Jagged1, which encodes a ligand for Notch1. Nat Genet. 1997; 16:243–251. [PubMed: 9207788]
29. Luxan G, et al. Mutations in the NOTCH pathway regulator MIB1 cause left ventricular noncompaction cardiomyopathy. Nat Med. 2013; 19:193–201. [PubMed: 23314057]
30. Chi NC, et al. Foxn4 directly regulates tbx2b expression and atrioventricular canal formation. Genes Dev. 2008; 22:734–739. [PubMed: 18347092]
31. Palencia-Desai S, et al. Vascular endothelial and endocardial progenitors differentiate as cardiomyocytes in the absence of Etsrp/Etv2 function. Development. 2011; 138:4721–4732. [PubMed: 21989916]
32. D'Amico L, Scott IC, Jungblut B, Stainier DY. A mutation in zebrafish hmgcr1b reveals a role for isoprenoids in vertebrate heart-tube formation. Curr Biol. 2007; 17:252–259. [PubMed: 17276918]
33. Kikuchi K, et al. Primary contribution to zebrafish heart regeneration by gata4(+) cardiomyocytes. Nature. 2010; 464:601–605. [PubMed: 20336144]
34. Kettleborough RN, et al. A systematic genome-wide analysis of zebrafish protein-coding gene function. Nature. 2013; 496:494–497. [PubMed: 23594742]
35. Huang CJ, Tu CT, Hsiao CD, Hsieh FJ, Tsai HJ. Germ-line transmission of a myocardium-specific GFP transgene reveals critical regulatory elements in the cardiac myosin light chain 2 promoter of zebrafish. Dev Dyn. 2003; 228:30–40. [PubMed: 12950077]
36. Thermes V, et al. I-SceI meganuclease mediates highly efficient transgenesis in fish. Mech Dev. 2002; 118:91–98. [PubMed: 12351173]

37. Mosimann C, et al. Ubiquitous transgene expression and Cre-based recombination driven by the ubiquitin promoter in zebrafish. Development. 2011; 138:169–177. [PubMed: 21138979]

38. Kwan KM, et al. The Tol2kit: a multisite gateway-based construction kit for Tol2 transposon transgenesis constructs. Dev Dyn. 2007; 236:3088–3099. [PubMed: 17937395]

39. Zhou Y, et al. Latent TGF-beta binding protein 3 identifies a second heart field in zebrafish. Nature. 2011; 474:645–648. [PubMed: 21623370]

40. Zhang R, et al. In vivo cardiac reprogramming contributes to zebrafish heart regeneration. Nature. 2013; 498:497–501. [PubMed: 23783515]

41. Yu PB, et al. Dorsomorphin inhibits BMP signals required for embryogenesis and iron metabolism. Nat Chem Biol. 2008; 4:33–41. [PubMed: 18026094]

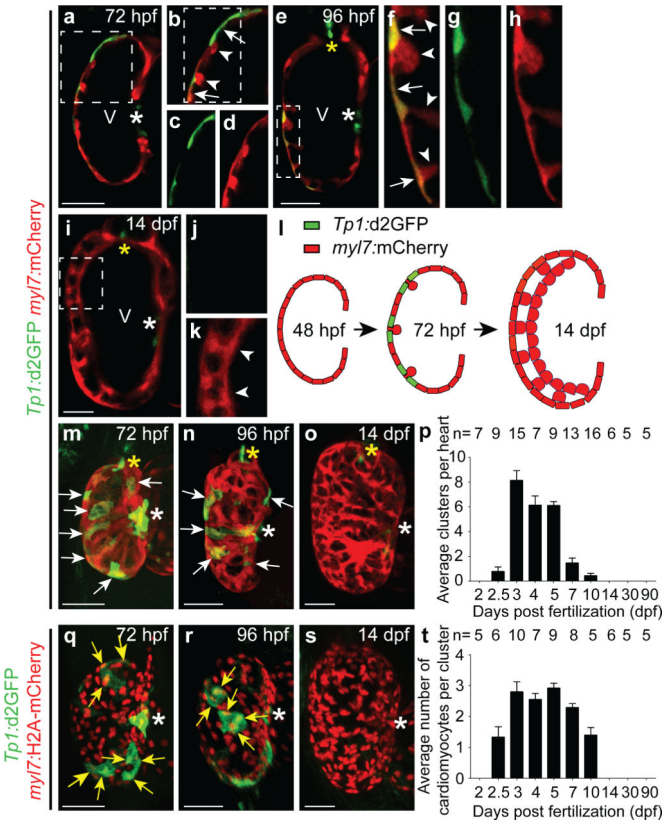


**Figure 1. Notch signaling is dynamically activated in distinct myocardial clusters during cardiac morphogenesis**

Cardiac ventricles at 72 hpf, 96 hpf and 14 dpf expressing **(a-k, m-o)** *Tp1:*d2GFP; *myl7:*mCherry or **(q-s)** *Tp1:*d2GFP; *myl7:*H2A-mCherry. **(a-k)** confocal slices, **(m-o, q-s)** 3D reconstructions. **b, c-d, f-h, j-k** insets are magnifications of **a, b, e, i,** boxed areas. **c-d, g-h, j-k** are single channels from **b, f, i** merged images. (**l**) Myocardial Notch signaling schematic. Quantification of (**p**) myocardial *Tp1:*d2GFP$^{+}$ clusters and (**t**) cardiomyocytes per *Tp1:*d2GFP$^{+}$ cluster. n – number of embryos analyzed per stage. White arrows – *Tp1:*d2GFP$^{+}$ cardiomyocytes, white arrowheads – trabeculating cardiomyocytes, and yellow arrows – cardiomyocytes in *Tp1:*d2GFP$^{+}$ clusters. White and yellow asterisks - AV and OFT. Mean +/− s.e.m. Scale bar 25 μm.

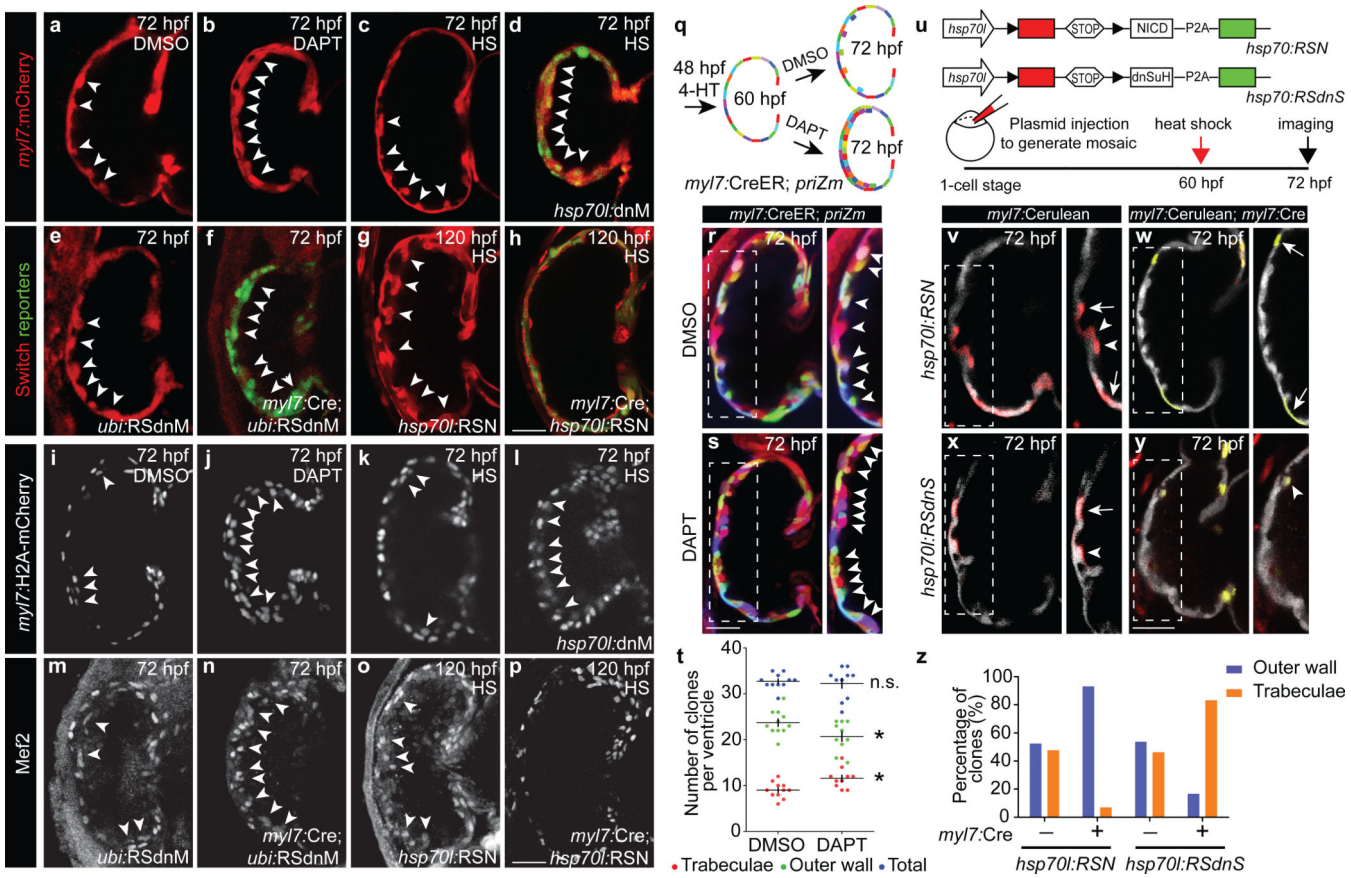


**Figure 2. Myocardial Notch signaling cell-autonomously regulates cardiomyocyte segregation between ventricular wall layers**

Inhibiting Notch signaling by (**b, j**) DAPT treatment; (**d, l**) global dnMAML-GFP (*hsp70l:*dnM); or (**f, n**) myocardial-specific dnMAML expression (*myl7:*Cre; *ubi:*RSdnM) leads to excessive trabeculation at 72 hpf, whereas (**h**, **p**) myocardial-specific constitutive Notch activation via NICD expression (*myl7:*Cre*; hsp70l:*RSN) diminishes trabeculation at 120 hpf. **a, c, e, g, i, k, m, o** panels represent respective controls for each condition. (**a-p**) For quantification see Extended Data Figure 5. (**q**) Myocardial *priZm* (brainbow) clonal studies. (**r, s**) 72 hpf *myl7:*CreER; *priZm* myocardial clones treated with DMSO or DAPT at 60 hpf. (**t**) Although DMSO and DAPT-treated ventricles display a similar overall number of myocardial clones (blue) (n = 10 and 11 embryos), DAPT-treated ventricles exhibit more clones in trabeculae (red) and less in the outer ventricular wall (green), compared with control. Crosses – mean and s.e.m. *$p < 0.05$, by Student's *t*-test. n.s. – not significant. **(u)** Notch-altering mosaic cardiomyocyte studies. (**w**) Constitutively-activated Notch cardiomyocytes expressing NICD-P2A-Emerald are primarily located on the ventricular outer wall (n = 13/14 clones, Fisher's exact test, $p < 0.05$); whereas (**y**) Notch-inhibited cardiomyocytes expressing dnSuH-P2A-Emerald are mainly found in trabeculae (n = 15/18 clones, Fisher's exact test, $p < 0.05$). **(v, x)** In controls lacking *Tg(myl7:cre),* mCherry$^{+}$ cardiomyocytes are distributed equally between both layers (n = 11/21 and 14/26 clones in the outer wall). (**z**) Quantitative analysis of **v-y.** Insets are magnifications of boxed areas.

Arrowheads and arrows – trabeculae and outer wall cardiomyocytes. HS – heat shock. Scale bar 25 μm.

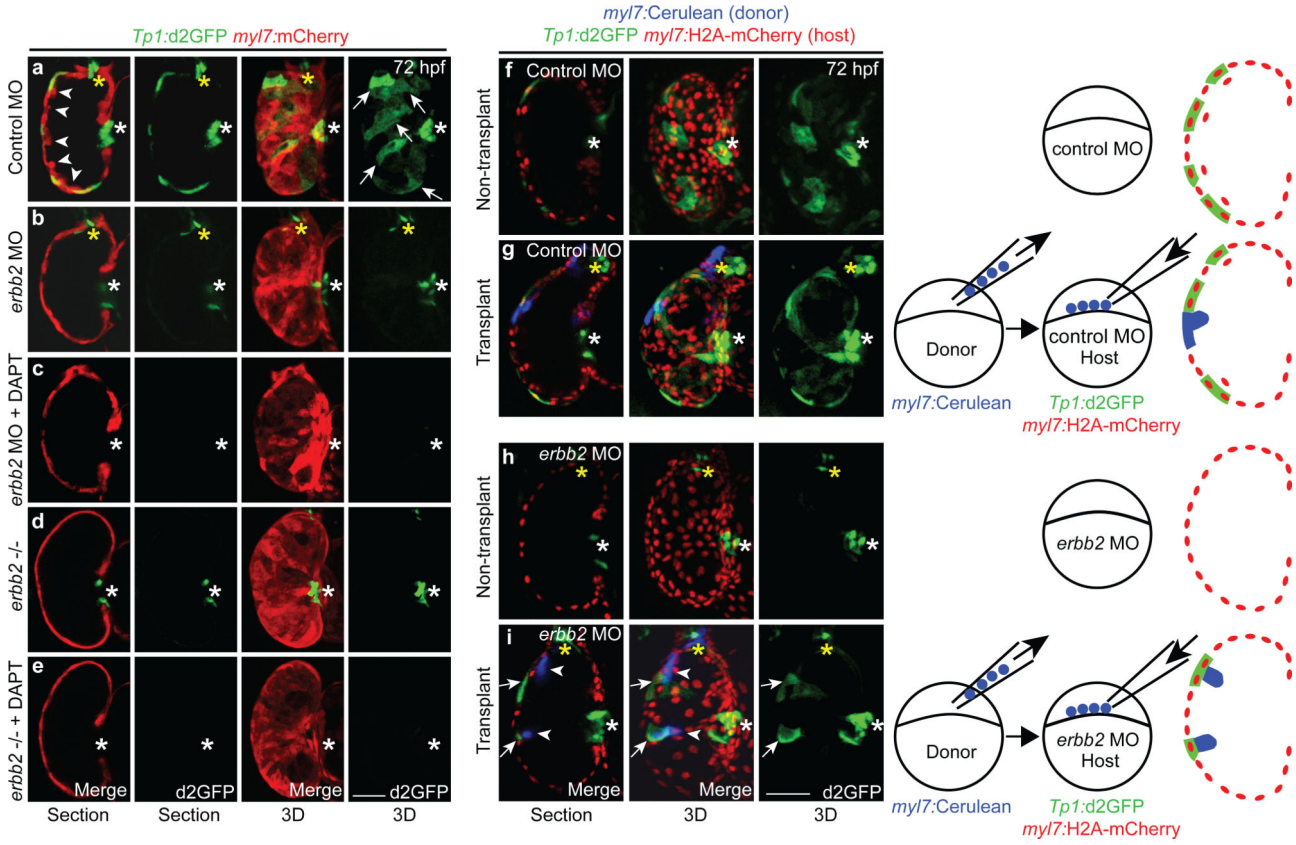


**Figure 3. Myocardial Erbb2 signaling non-cell-autonomously activates Notch signaling in neighboring cardiomyocytes**

Compared to (**a**) controls (n = 0/15 embryos), *Tp1*:d2GFP; *myl7*:mCherry (**b**) *erbb2* morpholino (MO) (n = 10/12) and (**d**) *erbb2* −/− mutants (n = 10/10) display reduced trabeculae and myocardial Notch signaling. (**c, e**) DAPT treatment at 60 hpf cannot rescue these myocardial defects, but can diminish AV and OFT endocardial Notch signaling (asterisks) (n = 15/17, 17/17 embryos, respectively). (**f-i**) Blastomere transplantation studies. Compared to (**g**) control MO hosts (n = 12 embryos), (**i**) a greater percentage of donor *Tg(myl7:Cerulean)* wild-type cardiomyocytes are located in the trabeculae of *erbb2* MO *Tg(Tp1:d2GFP; myl7:H2A-mCherry)* hosts (n = 10). In contrast to (**h**) non-transplanted *erbb2* MO hearts (n = 16), (**i**) transplanted donor *Tg(myl7:Cerulean)* wild-type cardiomyocytes (arrowheads) can activate myocardial Notch activity (*Tp1*:d2GFP) in neighboring *erbb2* MO *Tg(Tp1:d2GFP; myl7:H2A-mCherry)* host cardiomyocytes (arrows, n = 10). Scale bar 25 μm.

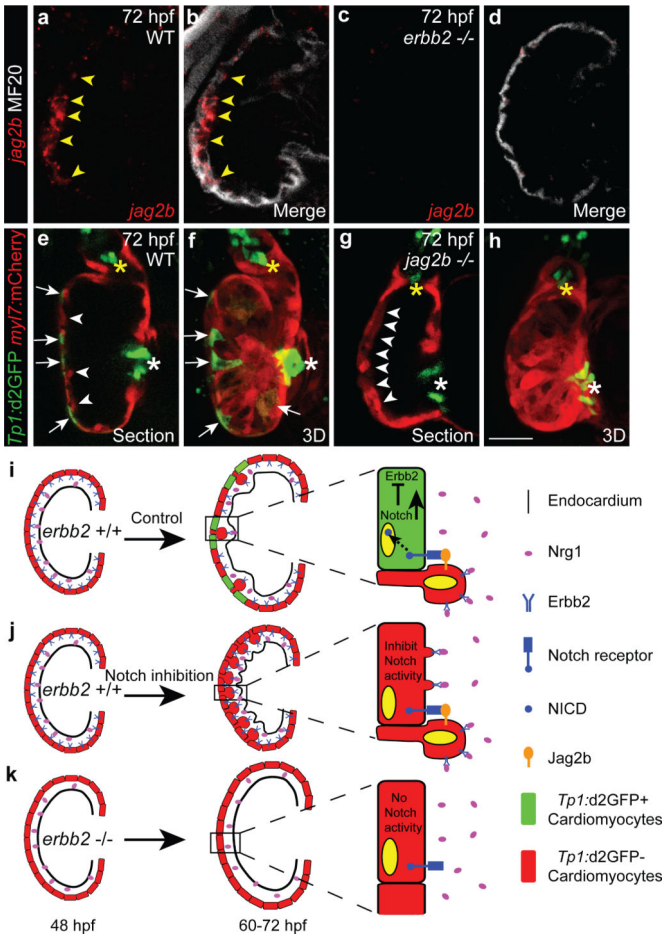


**Figure 4. The Notch ligand Jag2b mediates cooperative interactions between cardiomyocytes**

(**a-d**) *jag2b* is expressed in (**a, b**) wild-type (WT) (n = 6/6 embryos) but not (**c, d**) *erbb2* −/− mutant myocardium (MF20$^{+}$) (n = 0/5). (**e-h**) Compared to (**e, f**) WT controls (n = 0/10), (**g, h**) *Tg(Tp1:d2GFP; myl7:mCherry) jag2b* −/− mutants exhibit increased trabeculation and reduced myocardial Notch signaling at 72 hpf (n = 8/8). Yellow arrowheads – *jag2b*$^{+}$ cardiomyocytes; white arrowheads – trabeculae; white arrows – *Tp1:*d2GFP$^{+}$ cardiomyocytes; white and yellow asterisks – AV and OFT. Scale bar 25 μm. Myocardial Notch Signaling Model: (**i**) Endocardial Neuregulin/Nrg1 activates myocardial Erbb2 signaling, which cell-autonomously triggers myocardial sprouting and Jag2b expression (60-72 hpf). Jag2b activates Notch signaling in neighboring cardiomyocytes, which cell-autonomously inhibits *erbb2* expression and trabeculae formation (magnified area). (**j**) Inhibiting Notch signaling allows all cardiomyocytes to express *erbb2,* respond to Neuregulin, and sprout and form trabeculae. (**k**) Blocking Erbb2 signaling prevents trabeculation, Jag2b expression and Notch activation in neighboring cardiomyocytes.